December 1, 2020@CRFS

Research Progress in Gold Gratings and Gold-dielectric hybrid Gratings for Pulse Compressed

Jianda Shao, Yunxia Jin, Hongchao Cao,
Fanyu Kong, Yibin Zhang, Yonglu Wang,
Jiaolin Zhao, Kui Yi, Yuxing Han

SIOM
中国科学院上海光学精密机械研究所
Shanghai Institute of Optics and Fine Mechanics , CAS

Outline

1 Background and Challenge

2 Gold gratings

3 Gold-dielectric hybrid Gratings

4 Conclusion and acknowledge

Background

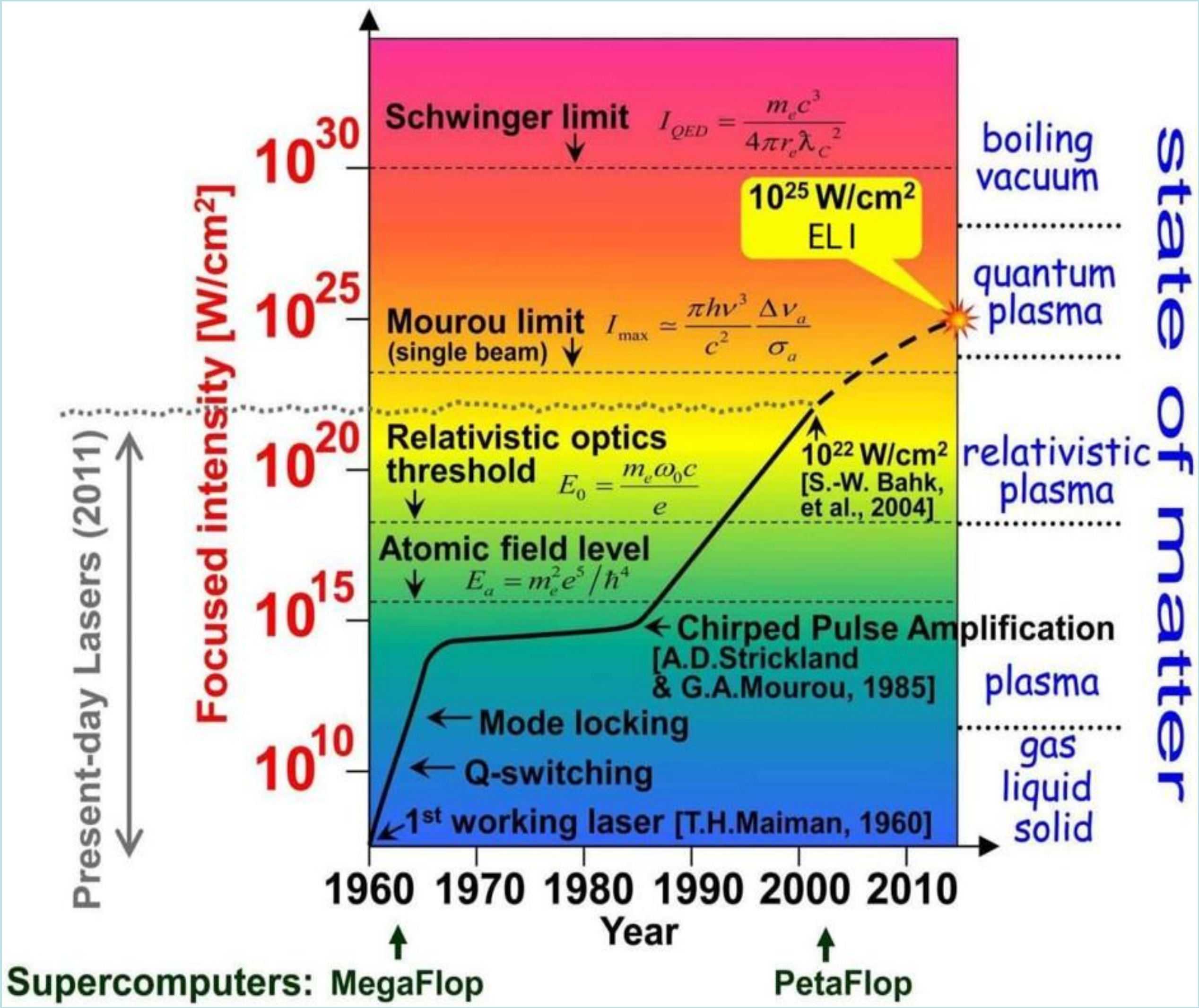

Intensity

& **Output energy(KJ)**

Pulse width(10's fs)

Focused size(μm)

Example:

10^{25}W/cm^2

=**1500J**/**15fs**/3.14μm^2

@910±100nm

- Optics & Photonics News, Gérard Mourou et.al.: “Relativistic Optics”-May-2004, “Extreme Light Infrasture: Optics Next Horizon”-July-2011

Background

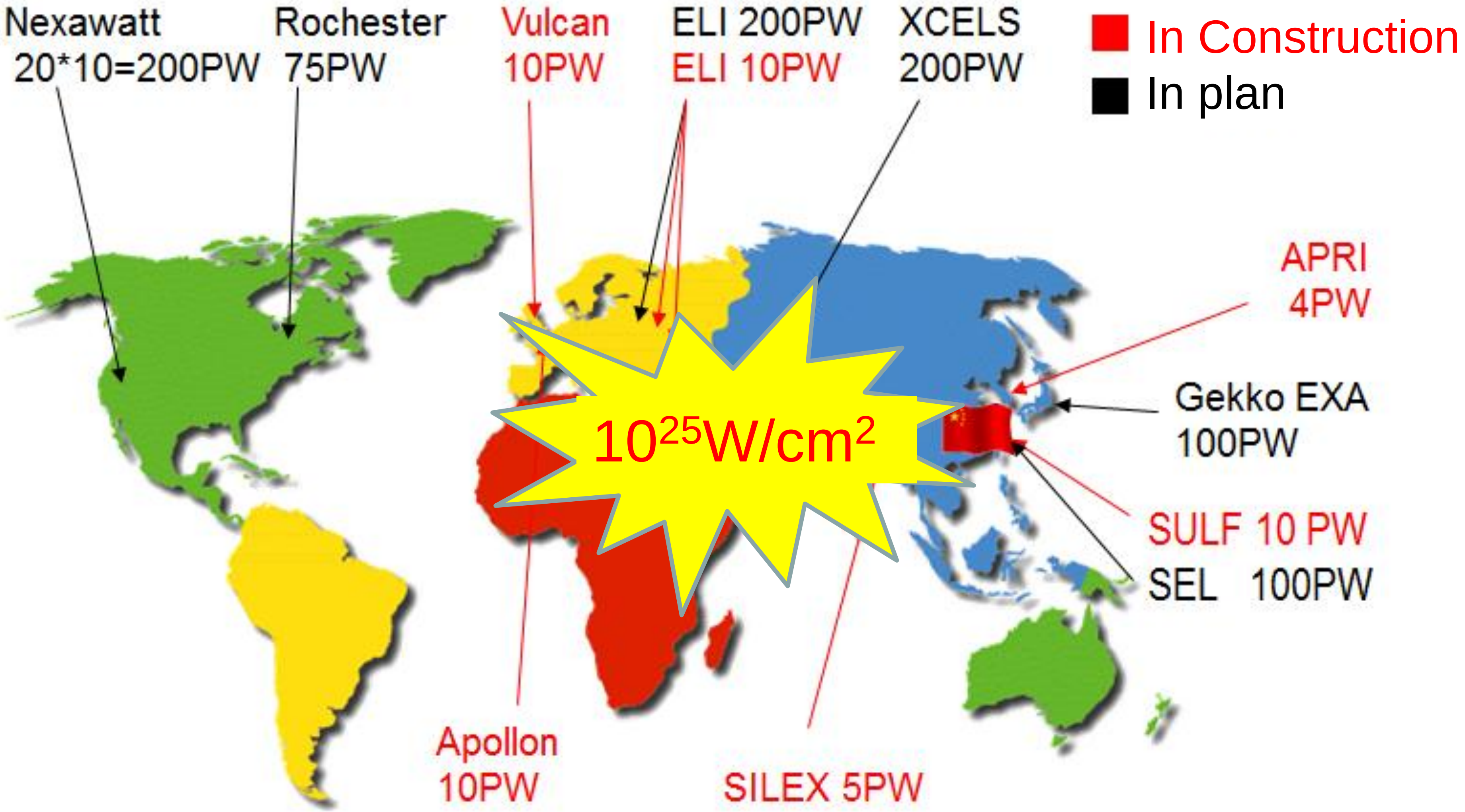
Nexawatt
20*10=200PW
Rochester
75PW
Vulcan
10PW
ELI 200PW
ELI 10PW
XCELS
200PW
🟥 In Construction
■ In plan
APRI
4PW
Gekko EXA
100PW
$10^{25}W/cm^2$
SULF 10 PW
SEL 100PW
Apollon
10PW
SILEX 5PW

Background

CPA research was done at University of Rochester in the mid 1980's

Chirped Pulse Amplifier

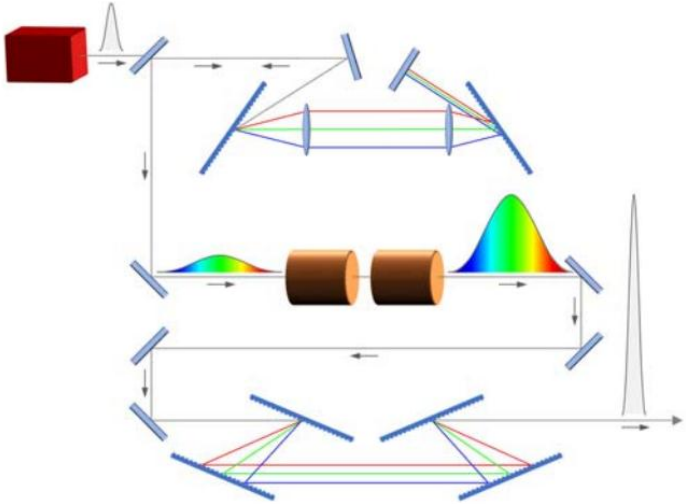

Pulse Compressed Gratings

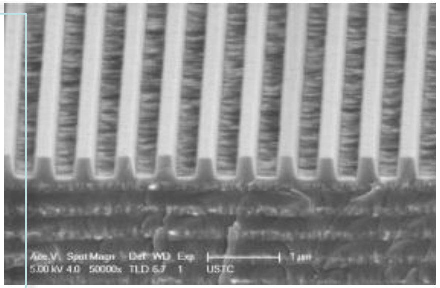

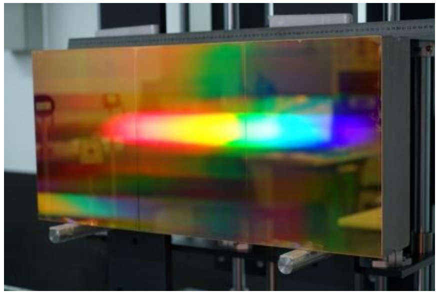

Background

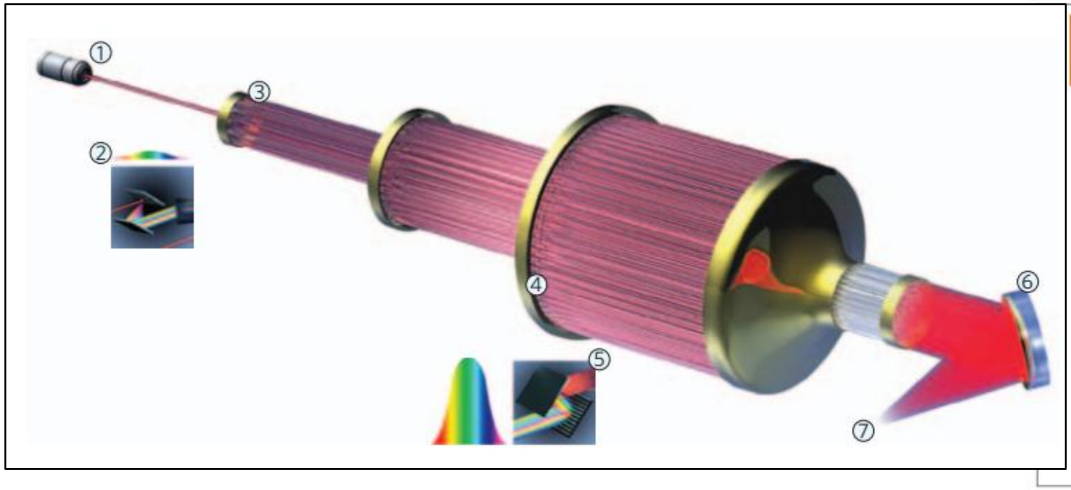

ELI 200PW

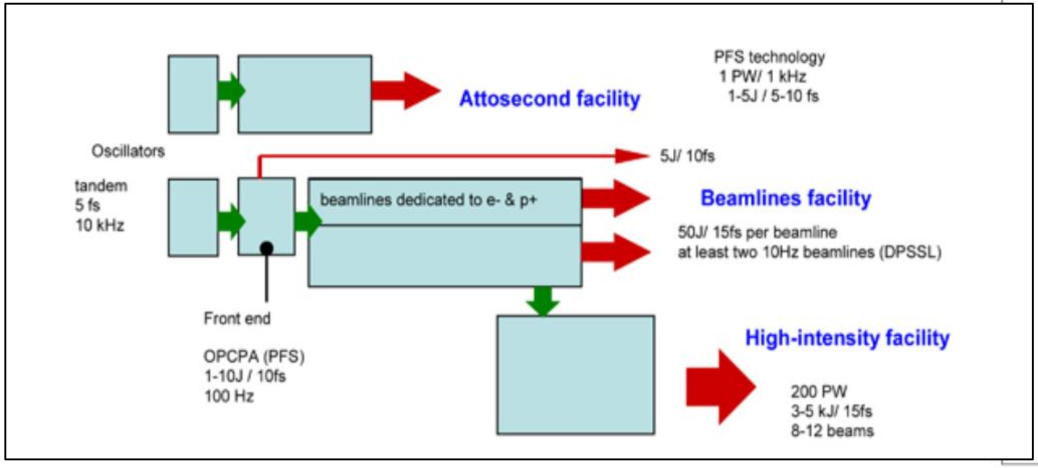

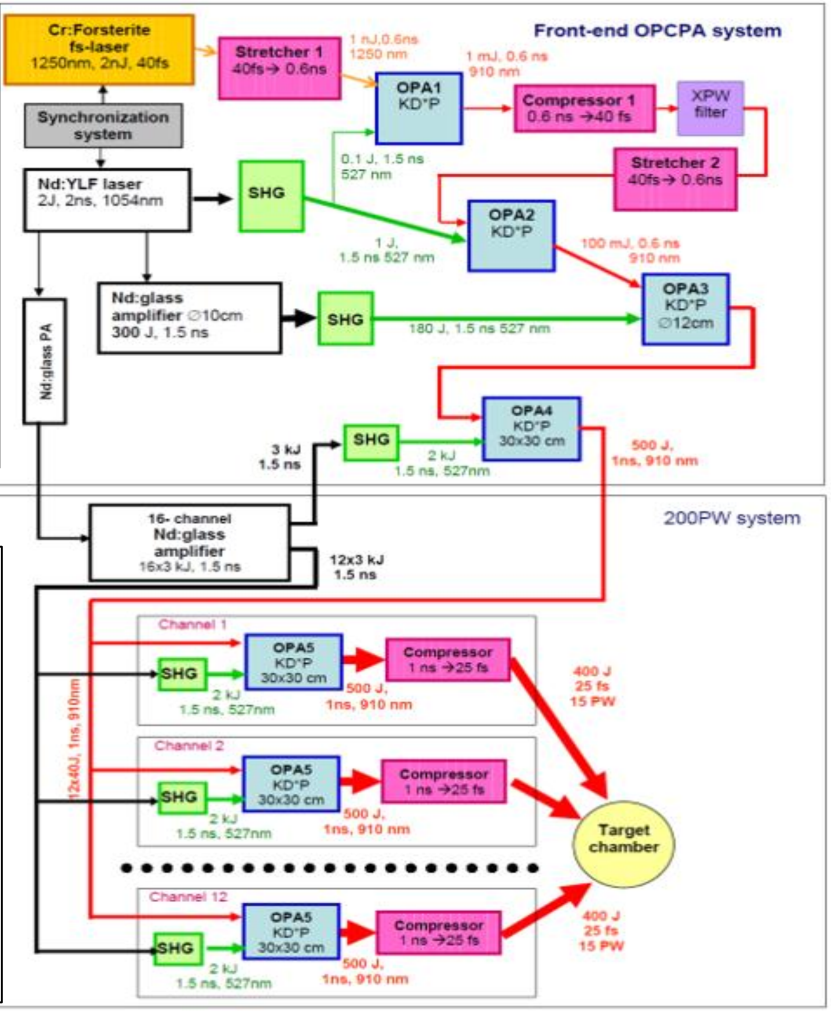

ELI 200PW & XCEL 200PW planed by coherent combining

Background

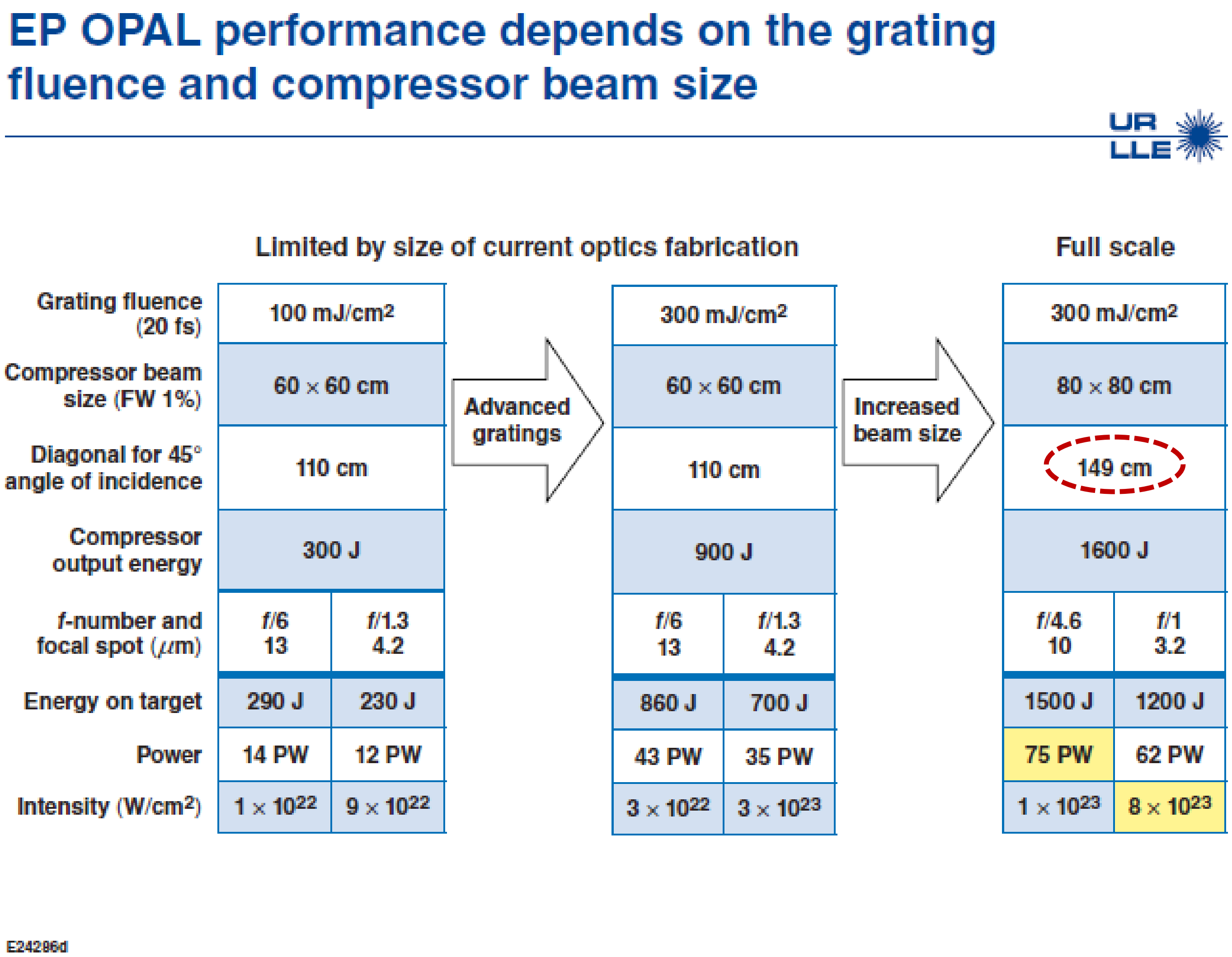

EP OPAL performance depends on the grating fluence and compressor beam size

	Limited by size of current optics fabrication				Full scale	
			Advanced gratings		Increased beam size	
Grating fluence (20 fs)	100 mJ/cm^2		300 mJ/cm^2		300 mJ/cm^2	
Compressor beam size (FW 1%)	60 × 60 cm		60 × 60 cm		80 × 80 cm	
Diagonal for 45° angle of incidence	110 cm		110 cm		149 cm	
Compressor output energy	300 J		900 J		1600 J	
f-number and focal spot (μm)	*f*/6 13	*f*/1.3 4.2	*f*/6 13	*f*/1.3 4.2	*f*/4.6 10	*f*/1 3.2
Energy on target	290 J	230 J	860 J	700 J	1500 J	1200 J
Power	14 PW	12 PW	43 PW	35 PW	75 PW	62 PW
Intensity (W/cm^2)	1 × 10^{22}	9 × 10^{22}	3 × 10^{22}	3 × 10^{23}	1 × 10^{23}	8 × 10^{23}

E24286d

75PW planed by single beam

Background

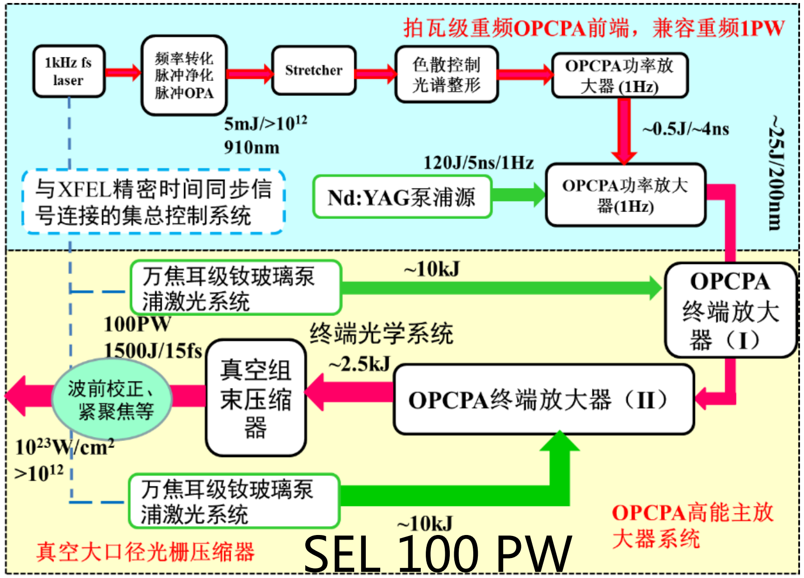

SEL 100 PW

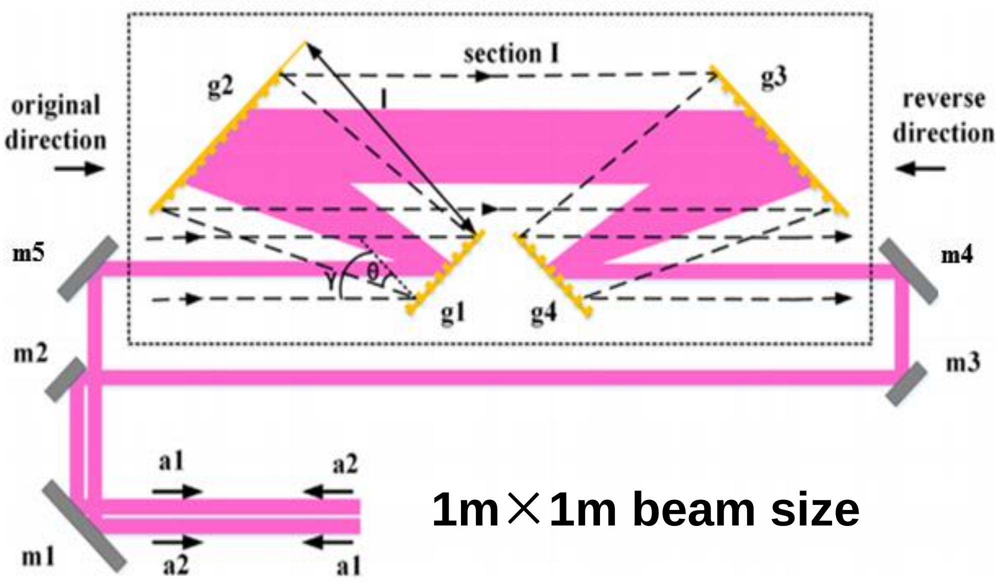

1m×1m beam size

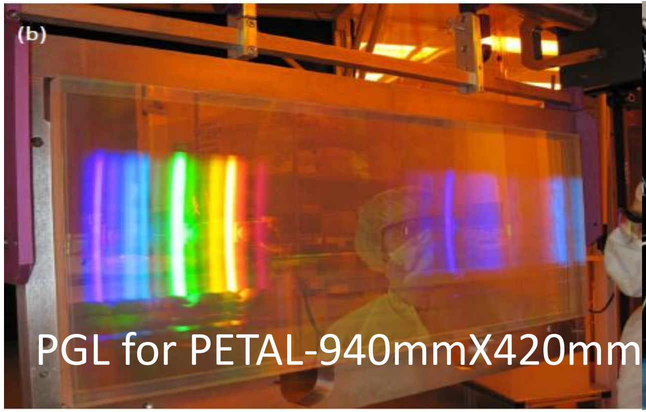

PGL for PETAL-940mmX420mm

LLNL, Φ940mm, 1480 L/mm

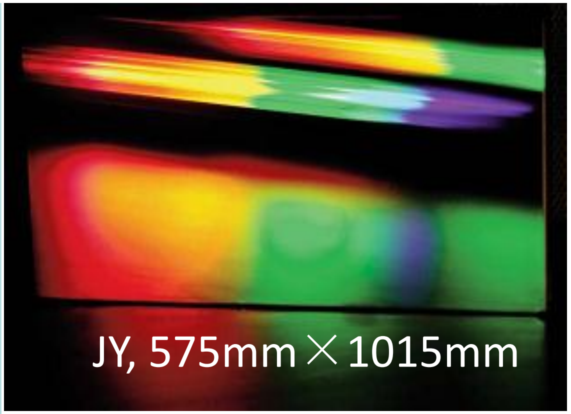

JY, 575mm×1015mm

Challenge

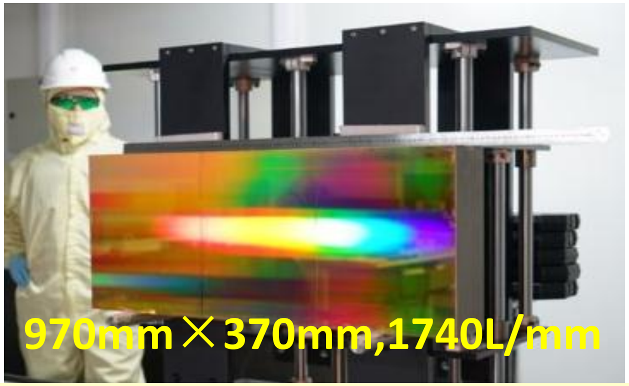
970mm×370mm,1740L/mm

China

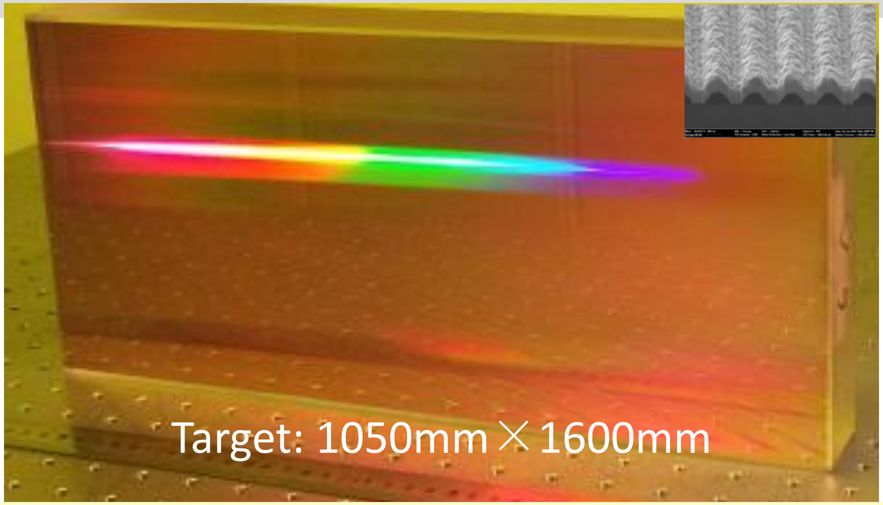
Target: 1050mm×1600mm

	requirements	laser performance	gratings
Spectrum bandwidth	≮200nm	15fs	±100nm
Diffractive efficiency	higher	low loss	>90%
Laser damage threshold	higher	transporting	≮0.2J/cm^2
Energy indurance	≮1500J	peak power	≮1600mm×1050mm

large&high-performance gratings related key technologys:

- Substrate polishing
- Thin-film optical coatings
- Pattering
- Reactive-ion etching
- Optical metrology and interaction of gratings and laser
- Precision cleaning,inspection,and handling large optics

Pulse Compression Gratings

Gold gratings:

☺ High diffraction efficiency

☺ Broad range of spectrum and deviation angles

√ Absorbing little % of incident light causing heating

Gold-Dielectric hybrid gratings:

☺ Even higher diffraction efficiency than gold

☺ Broader range of spectrum and angles than MLD gratings, maybe less than gold??

? Absorbing little incident light, but less than gold

MLD gratings:

☺ Highest diffraction efficiency of all reflection gratings

☺ Extremely low absorption

☻ Limitations on spectrum width and deviation angle range

Outline

02

PART TWO

Gold Gratings

Gold gratings' processing

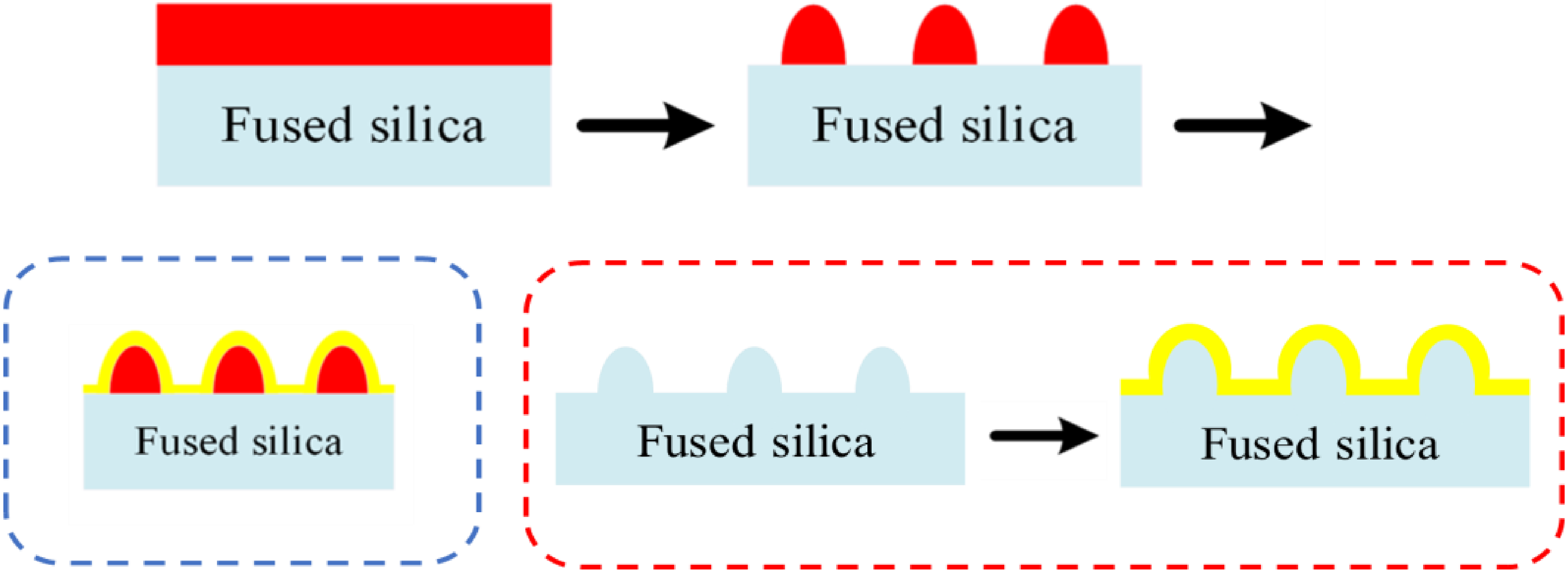

$$f(x) = h * \max\left[0, 1 - \left(\frac{\cos^2 \frac{\pi x}{d}}{\sin^2 \frac{\pi \Delta}{d}}\right)^{\sigma}\right], \qquad (\sigma > 0)$$

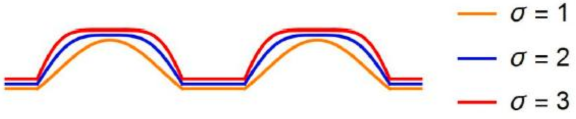

Research and fabrication at abroad

- LLNL and PGL，JY @800nm and 1053nm

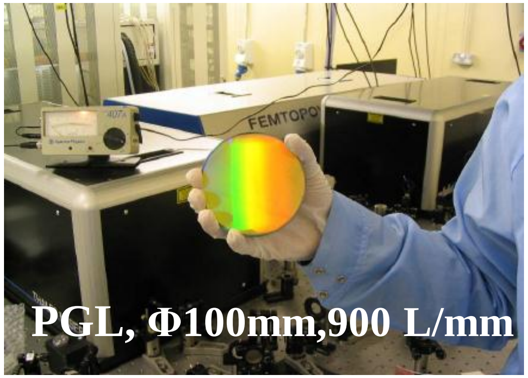

PGL, Φ100mm,900 L/mm

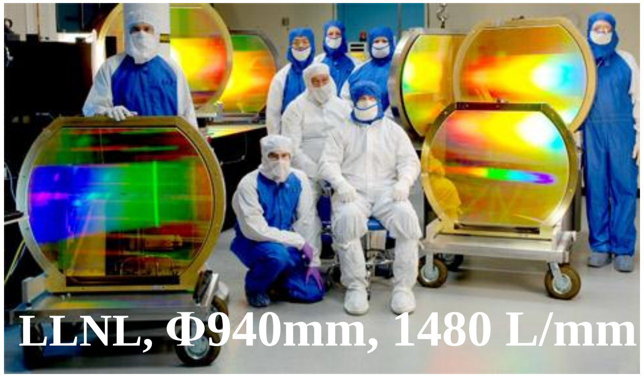

LLNL, Φ940mm, 1480 L/mm

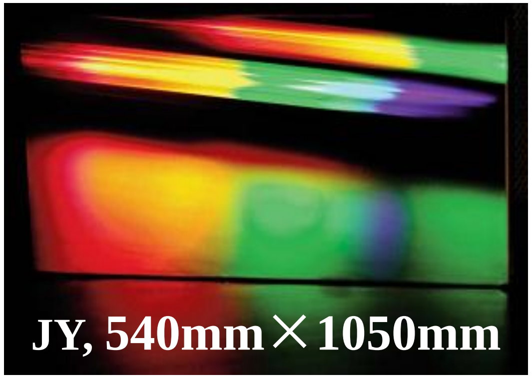

JY, 540mm×1050mm

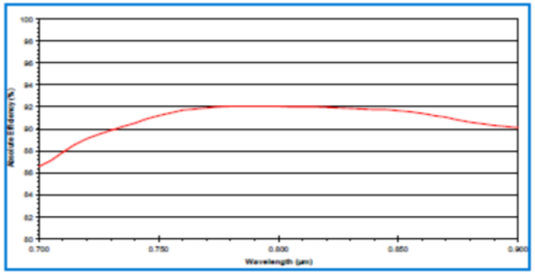

1480 g/mm, 800 nm, Dev=10°, inc. angle= 31.5°, TM, Au

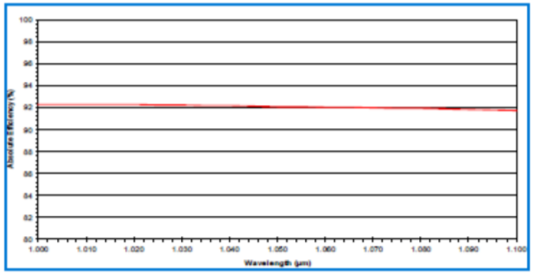

1480 g/mm, 1050 nm, Dev=10°, inc. angle=46.3°, TM, Au

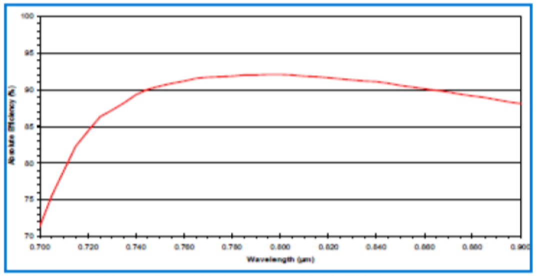

1200 g/mm, 800 nm, Dev=10°, inc. angle=23.8°, TM, Au

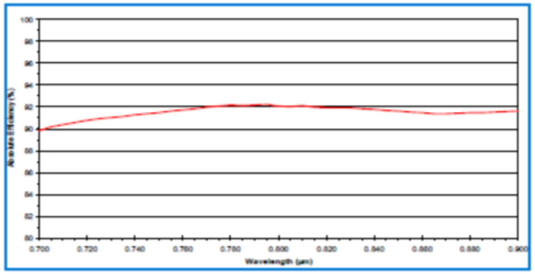

1740 g/mm, 800 nm, Dev=10°, inc. angle=39.3°, TM, Au

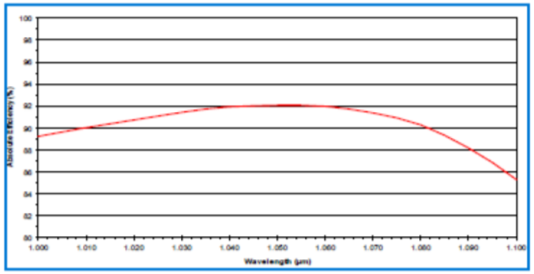

1740 g/mm, 1050 nm, Dev=10°, inc. angle=61.5°, TM, Au

NOTE:

These efficiency curves are absolute efficiencies, calculated using rigorous electromagnetic theory, and taking into account the true groove profiles of manufactured gratings measured with AFM microscope. They are typical and representative of the grating efficiency with an uncertainty band of ± 3%.

Laser induced damage

Journal of the Optical Society of America. B, Optical physics 13, 459 (1996)

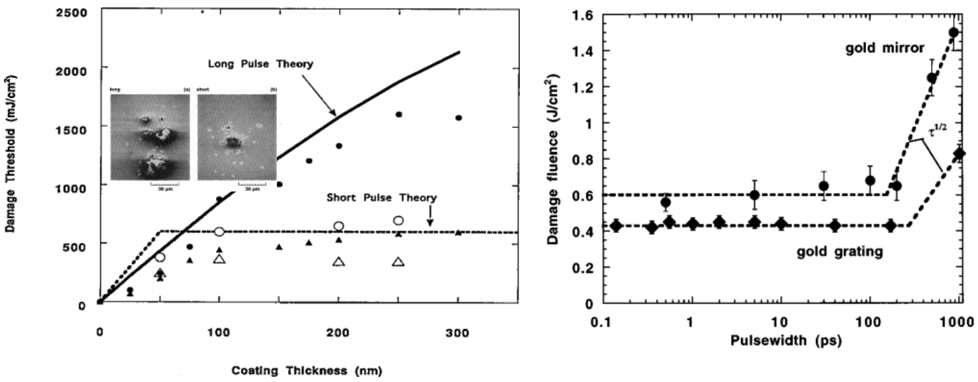

Fig. (a) Coating thickness dependence of damage threshold;
(b) pulse-width dependence of damage threshold.

Opt Express **21**, 26341 (2013)

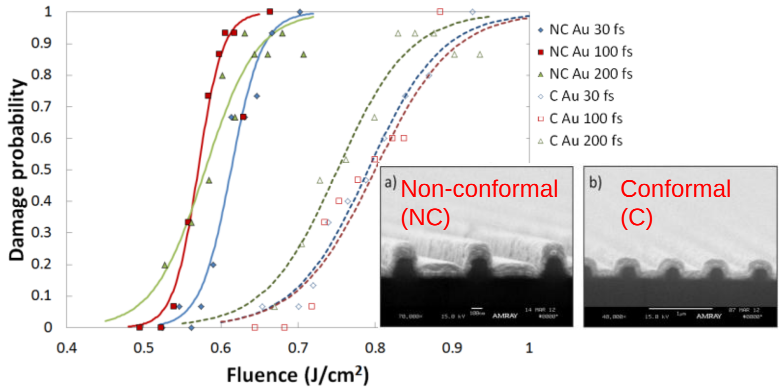

Fig. Pulse width dependence of damage threshold by different groove structure samples , from Plymouth Grating Laboratory.

Opt Laser Eng 95, 42-51 (2017)

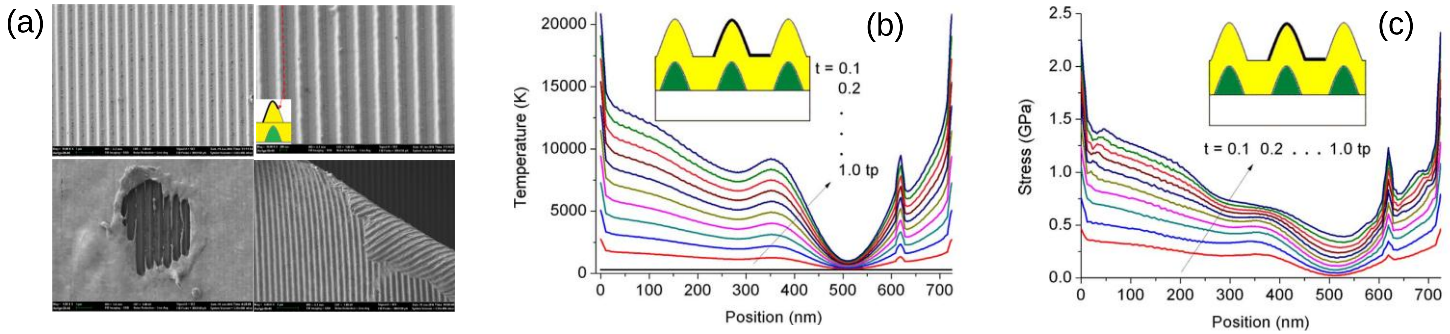

Fig. (a) Varied laser induced damage morphologies of gold coated gratings; (b)the surface temperature distribution; (c) the surface stress distribution of gold coated gratings in different time during laser irradiation.

- A linear dependence on **film thickness** to near the penetration depth in the short-pulse regime;
- The threshold nearly independent of the **pulse duration** in the short-pulse regime;
- The **conformal (C) coating** with a higher damage threshold than the non-conformal (NC) coating;
- The possible **damage drivers**: electron hydrodynamic pressure, thermal ablation and thermal stress.

Research and fabrication at home

- Design：1480 line/mm MG with Au grating layer for ~15fs compressed
  - DE>90% @800nm±75nm, 54° incident
  - DE>90% @910nm±100nm, 62° incident
  - Structure materials: Au + photoresist

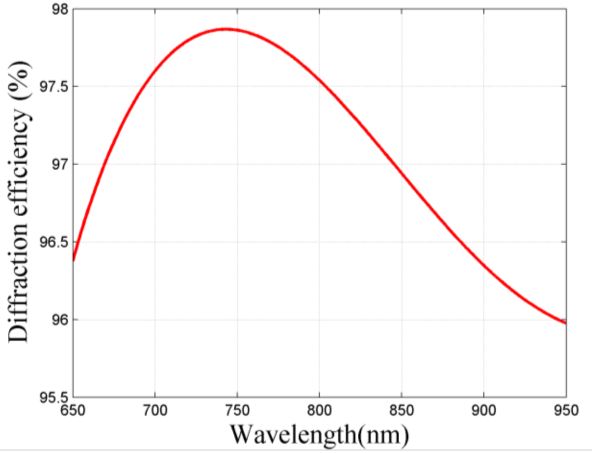

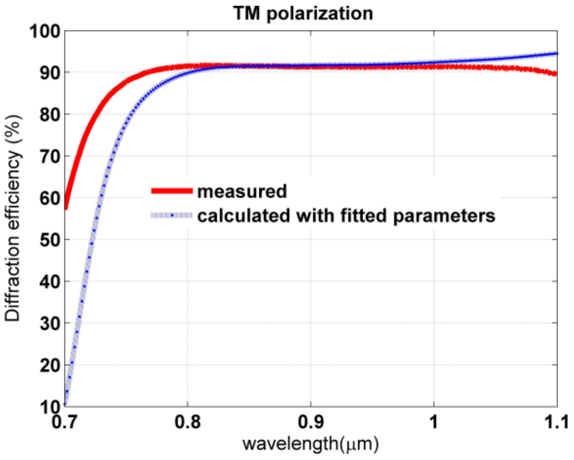

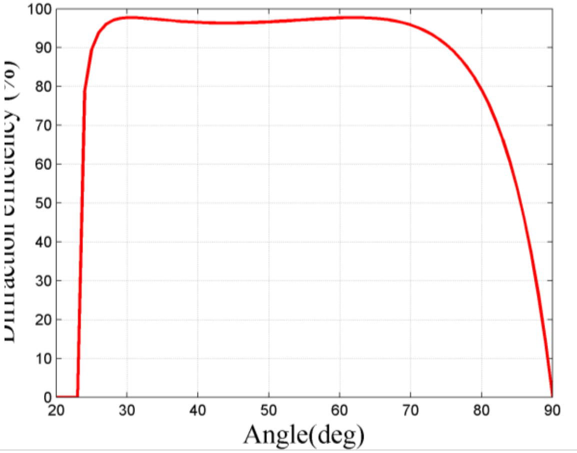

Laser induced damage threshold tests

ISO 21254-2011

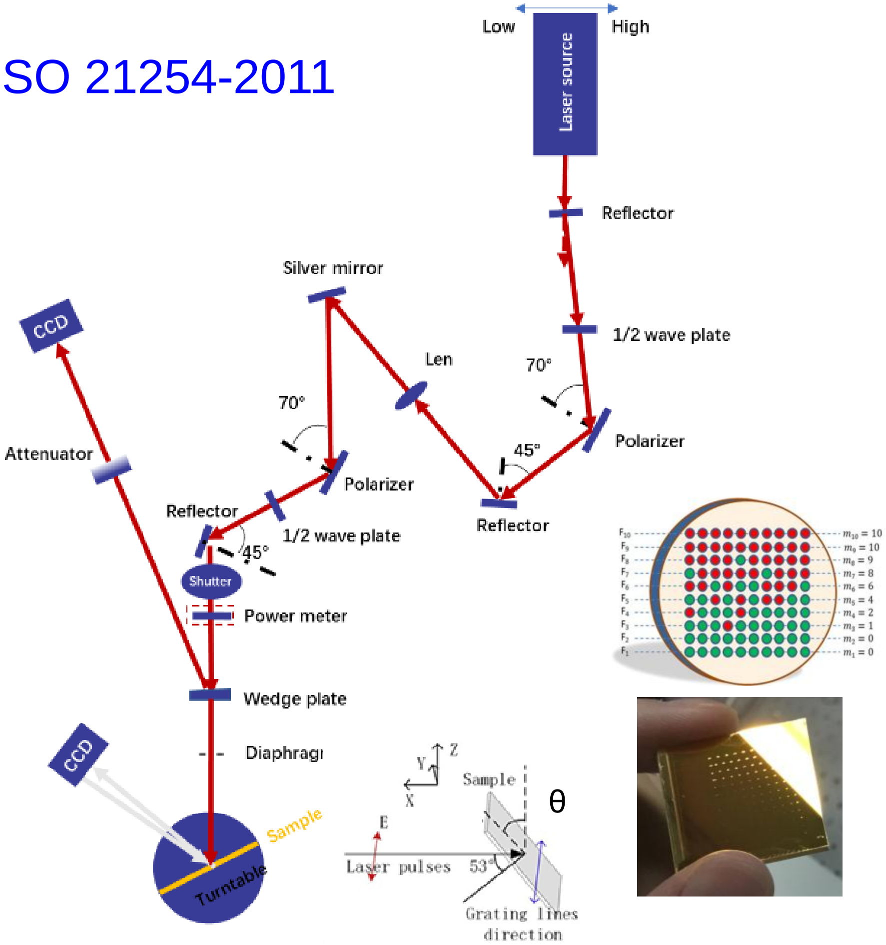

F(on grating surface) = F(on normal beam)×cosθ

Fig. Experimental setup for LIDT tests.

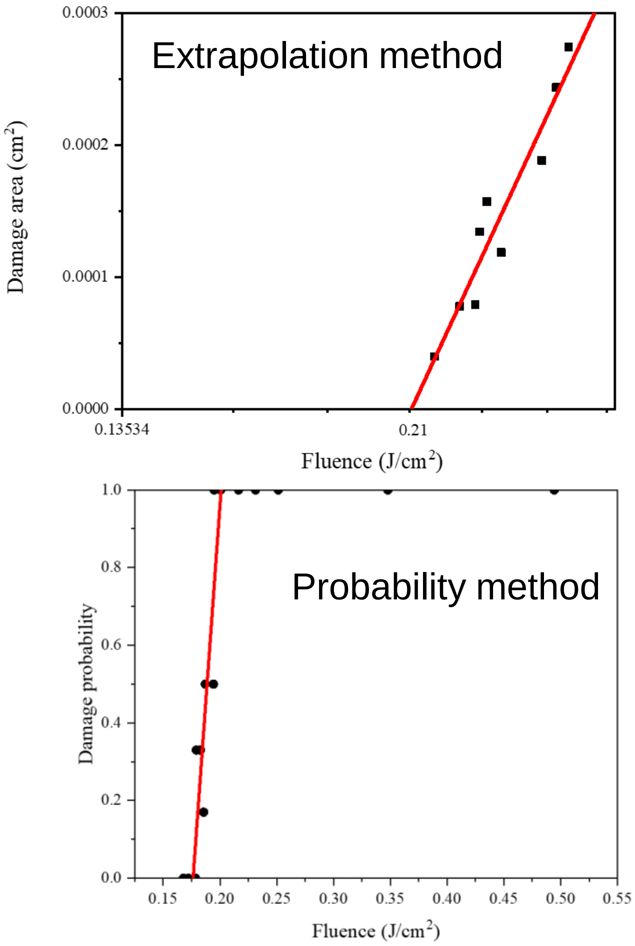

Fig. LIDT-calculation methods.

- Standard tests meeting the ISO LIDT protocol and proper assessments for different gratings and conditions.

1-on-1 laser induced damage morphology analysis

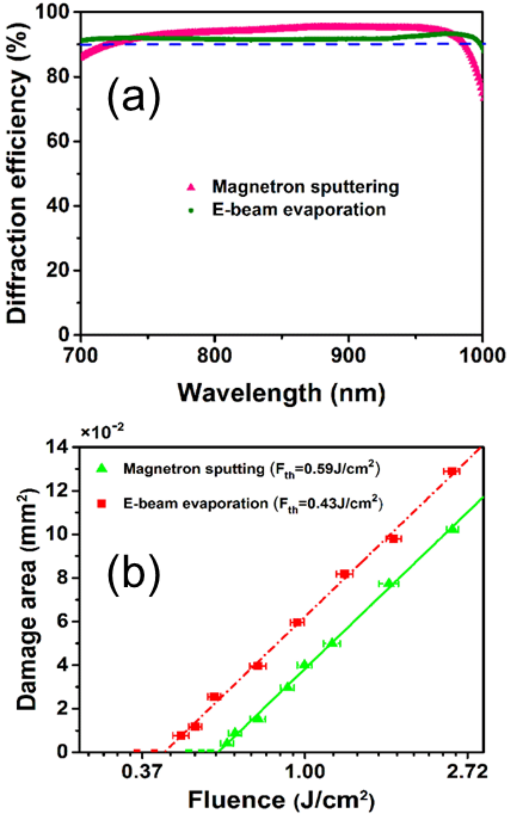

Fig. (a) Measured −1st-order diffraction efficiency; (b) LIDT with a pulse width of 60 fs.

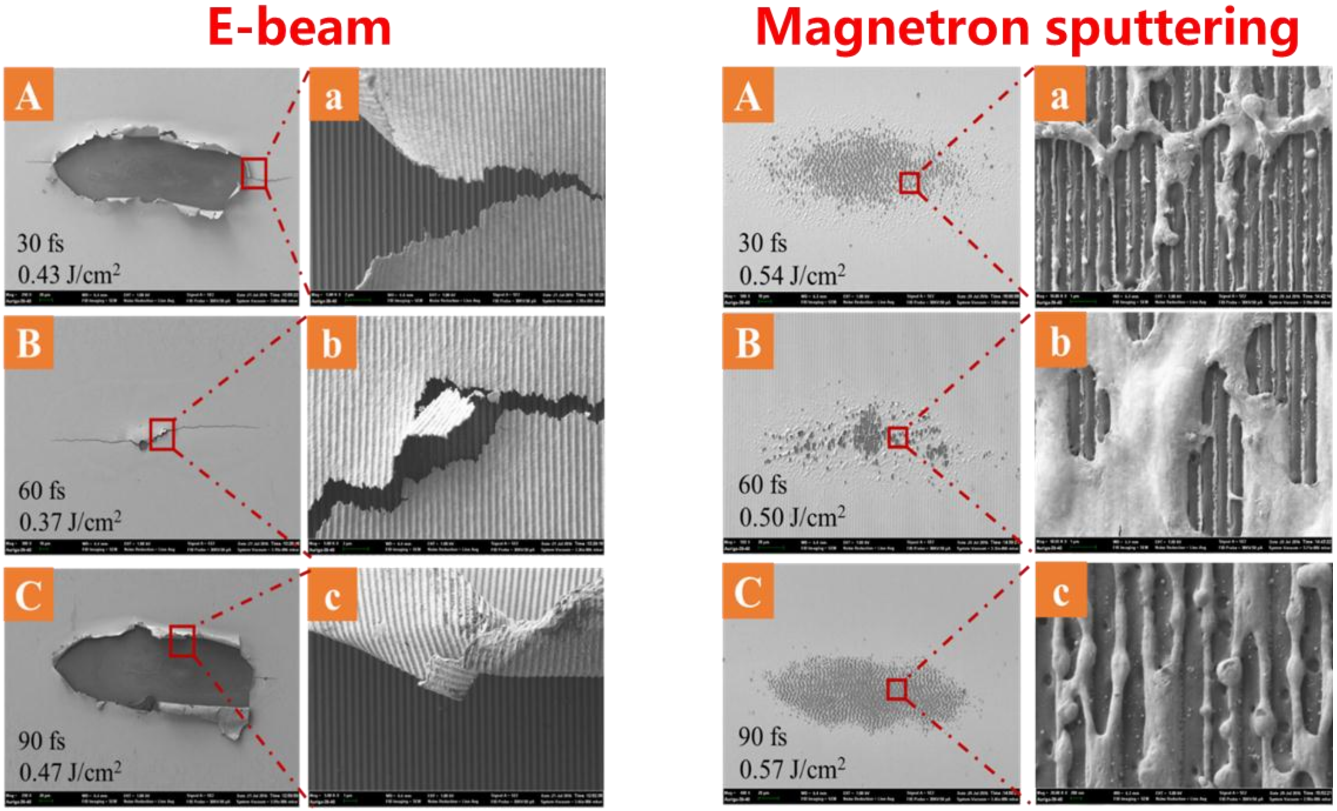

Fig. Typical damage morphologies of gold gratings fabricated by e-beam evaporation and magnetron sputtering at several laser fluences.

Applied Optics 56(11):3087 (2017)

- Gold deposited by e-beam: blister from stress-induced
- Gold deposited by sputtering: thermal fusion damage

Incubation effects

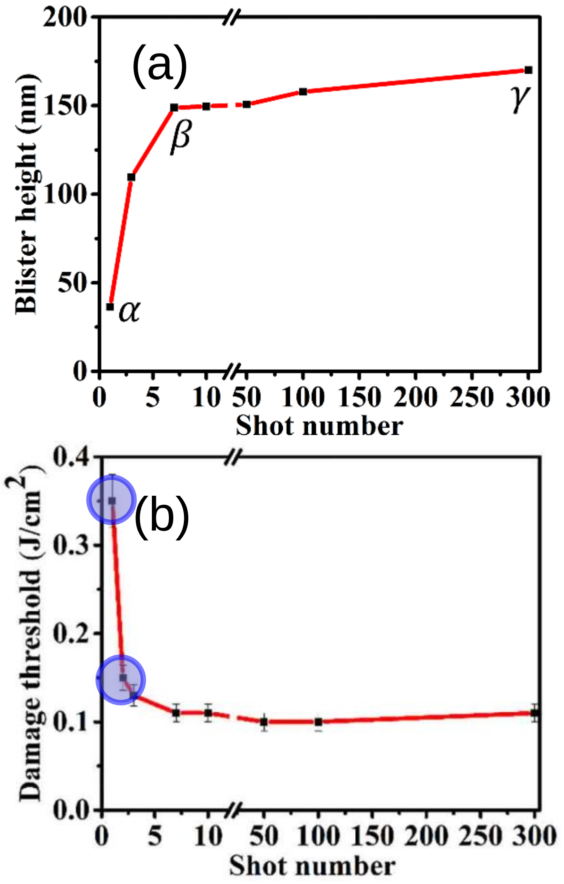

Fig. (a) Blister height information for different shots; (b) the evolution of LIDT versus shot number.

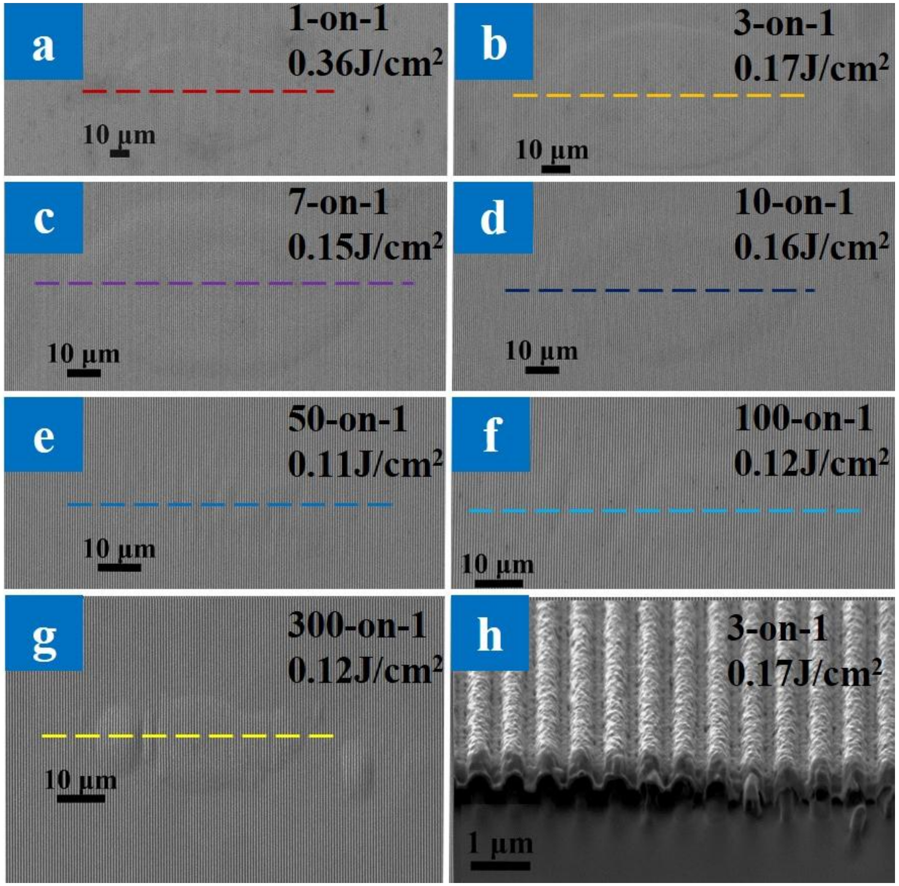

Fig. SEM images of typical blister with different number shots near the damage threshold and a FIB cross-section picture.

Optical Materials 72:130-135 (2017)

- The 2-on-1 LIDT decreased 60% compared to the 1-on-1 LIDT (1kHz).

Adhesion force comparation

Magnetron sputtering

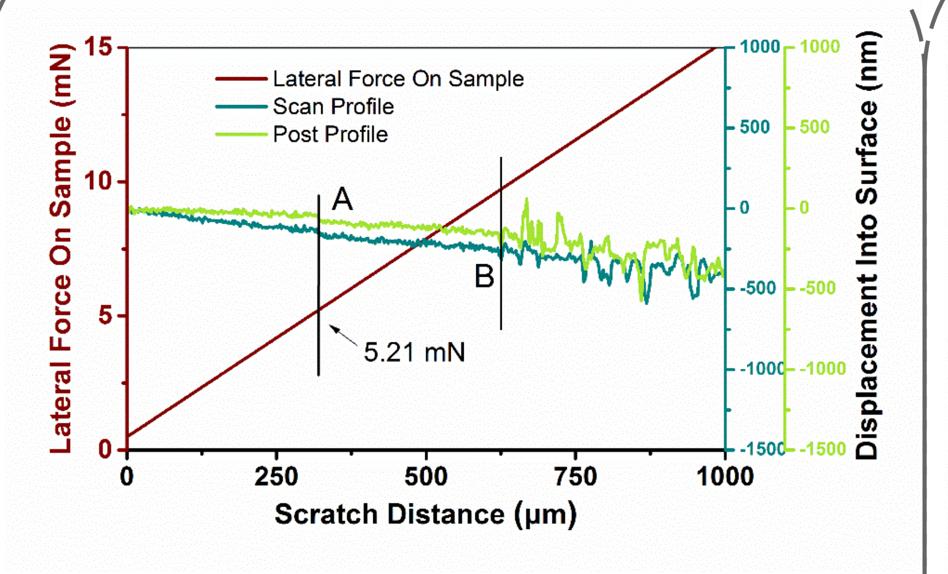

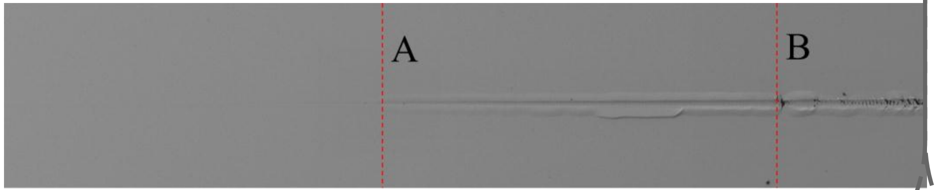

The adhesion forces: 5.21 *mN*

E-beam

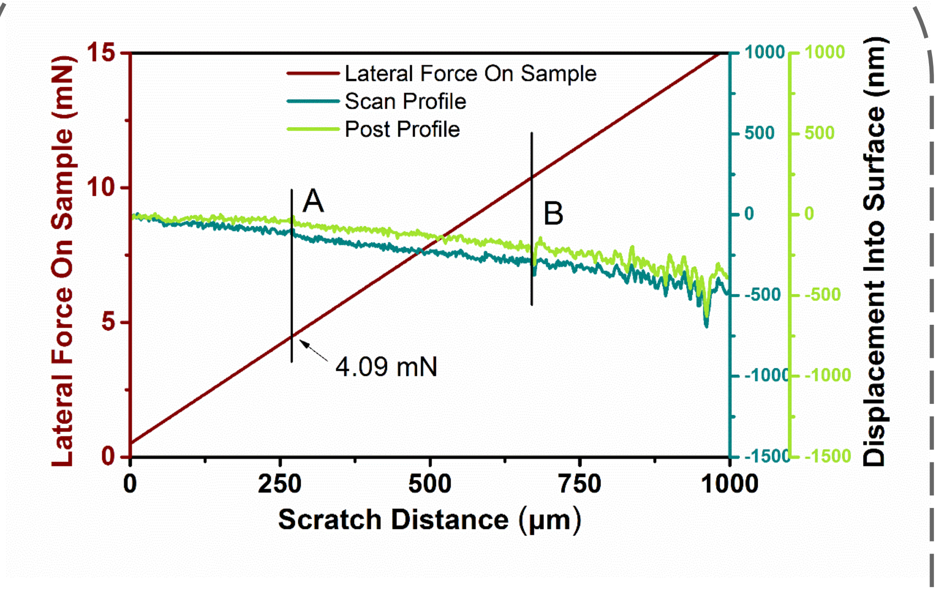

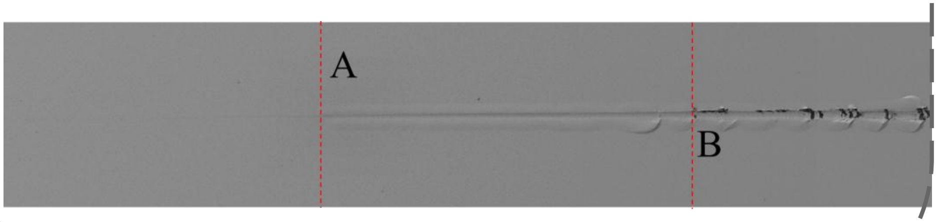

The adhesion forces: 4.09 *mN*

- Adhesion force comparation of different coating deposition method

Damage mechanism analysis

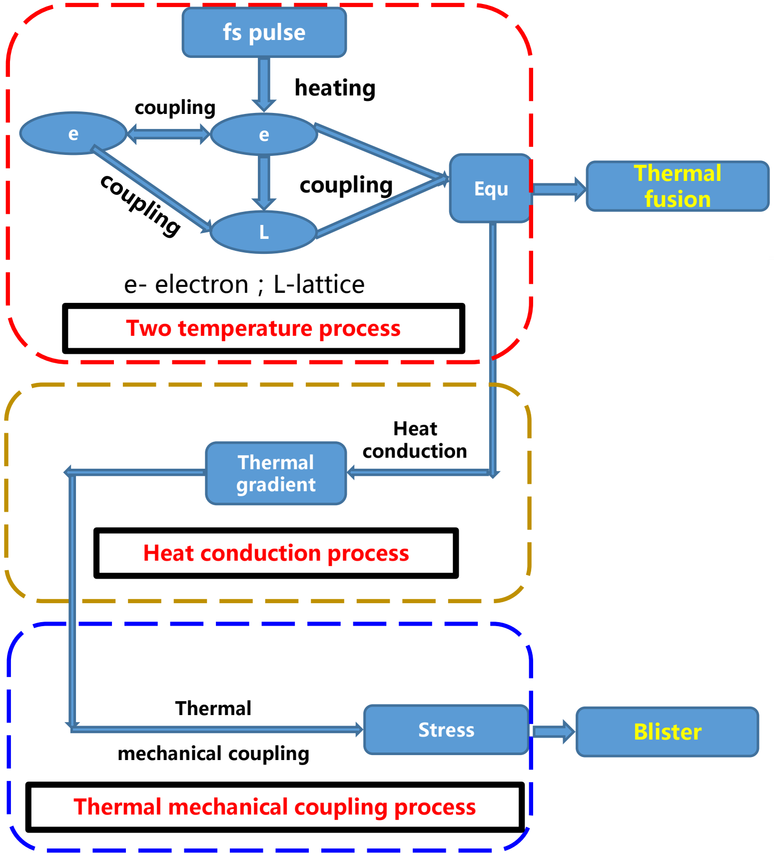

fs pulse

heating

coupling

e

e

coupling

coupling

L

Equ

Thermal fusion

e- electron；L-lattice

Two temperature process

Heat conduction

Thermal gradient

Heat conduction process

Thermal

mechanical coupling

Stress

Blister

Thermal mechanical coupling process

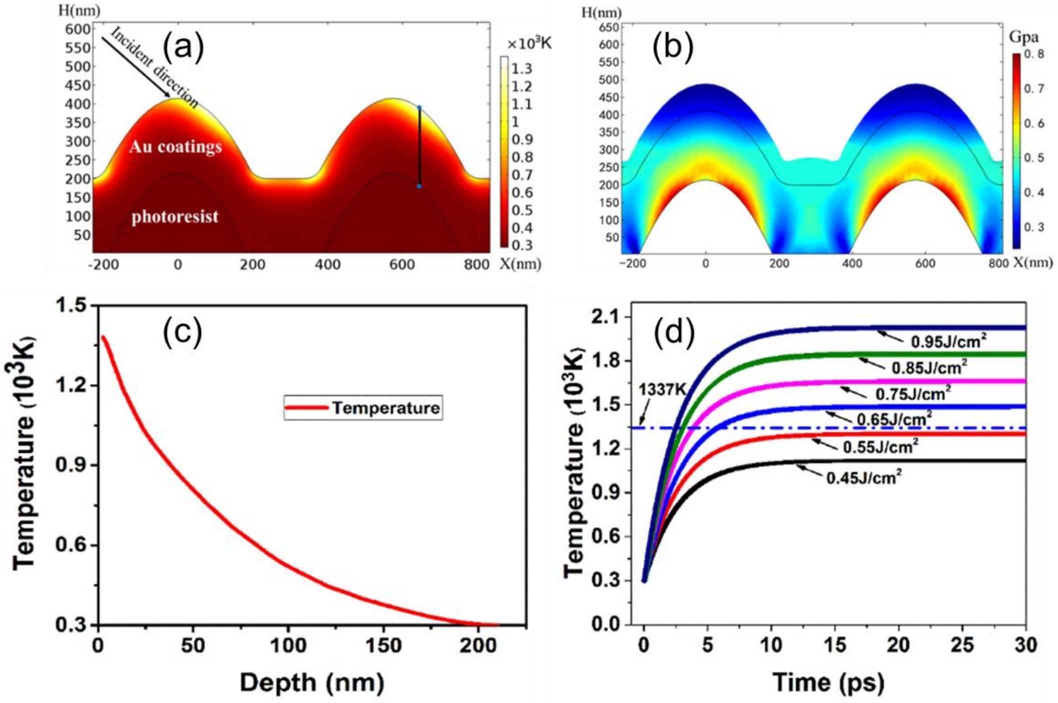

Fig. Thermal field and stress field simulation. (a) Temperature distribution; (b) thermal stress distribution; (c) temperature distribution in the vertical direction; (d) final surface temperature at different fluences.

Applied Optics 56(11):3087 (2017)

- The major factor of LID: the weak adhesion strength between the gold film and the photoresist.
- Explore better processes and structures to enhance the adhesion strength.

1480l/mm gold gratings

- 200mm×150mm
- 1480l/mm@910nm±100nm, 15 fs, 2019

元件编号	PV(λ=**632.8**nm)		
	+1级	0级	-1级
8#	0.480	0.099	0.517
10#	0.508	0.371	0.518
12#	0.521	0.116	0.570
14#	0.521	0.100	0.589

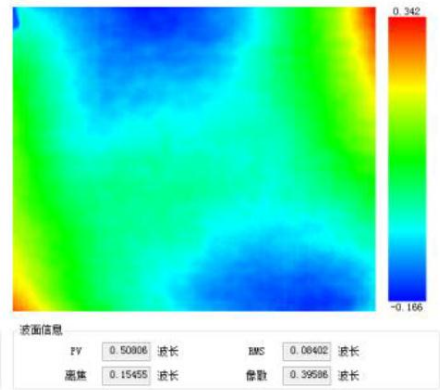

波面信息

PV 0.50806 波长 RMS 0.08402 波长

离焦 0.15455 波长 像散 0.39586 波长

+1 级

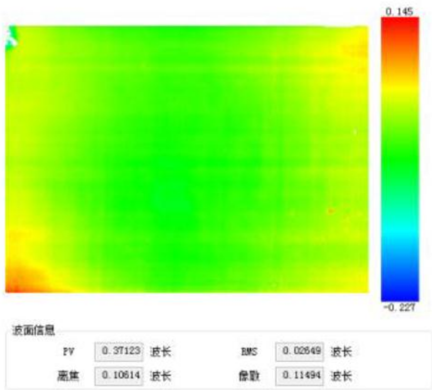

波面信息

PV 0.37123 波长 RMS 0.02649 波长

离焦 0.10614 波长 像散 0.11494 波长

0 级

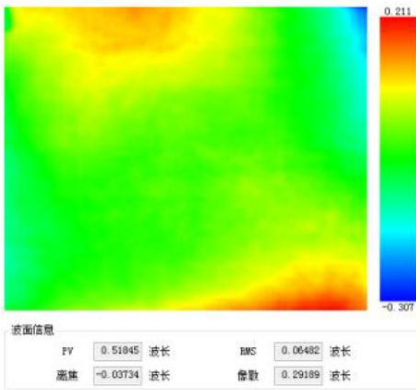

波面信息

PV 0.51845 波长 RMS 0.06482 波长

离焦 -0.03734 波长 像散 0.29189 波长

-1 级

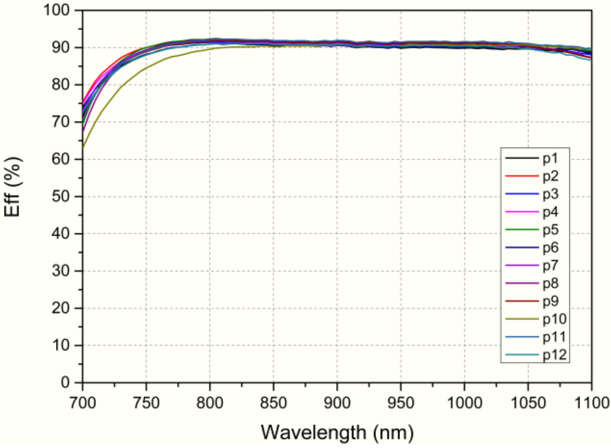

- new pattering technique proved

1480l/mm gold gratings

- 200mm×150mm
- 1480l/mm@910nm±100nm, 15fs，2020

元件编号	PV(λ=**632.8**nm)		
	+1级	0级	-1级
1905-200S-0501#	0.405	0.054	0.460
1905-200S-0503#	0.395	0.058	0.391
1905-200S-0504#	0.372	0.062	0.398
1905-200S-0506#	0.427	0.056	0.443

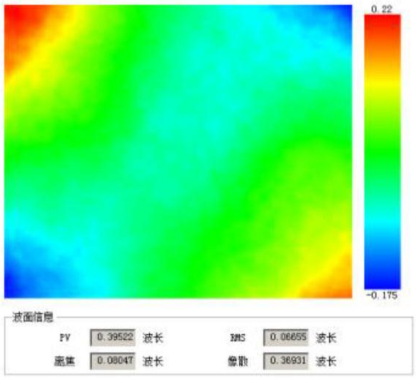

波面信息
PV 0.39522 波长 RMS 0.06655 波长
离焦 0.08047 波长 像散 0.36931 波长

+1 级

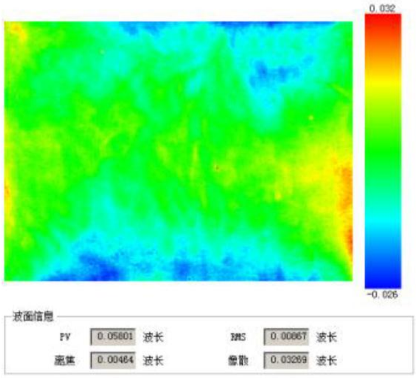

波面信息
PV 0.05801 波长 RMS 0.00667 波长
离焦 0.00464 波长 像散 0.03269 波长

0 级

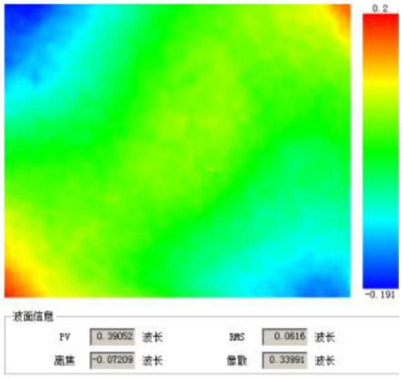

波面信息
PV 0.39052 波长 RMS 0.0616 波长
离焦 -0.07209 波长 像散 0.33991 波长

-1 级

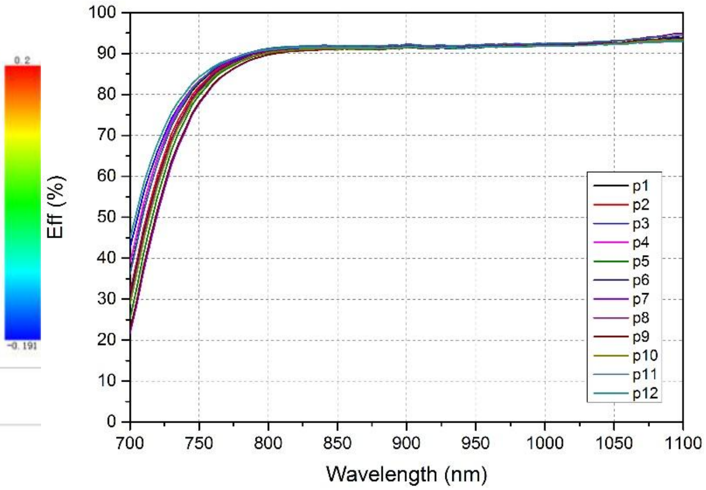

- new pattering technique proved

Application and LIDT

Testing Parameters：
Central wavelength：800nm
Repetition rate：1kHz
Polarization：TM
incident angle：53°
Pulse width：35±5fs
Effective area：0.14mm2
Gratings size: 200mm×150mm

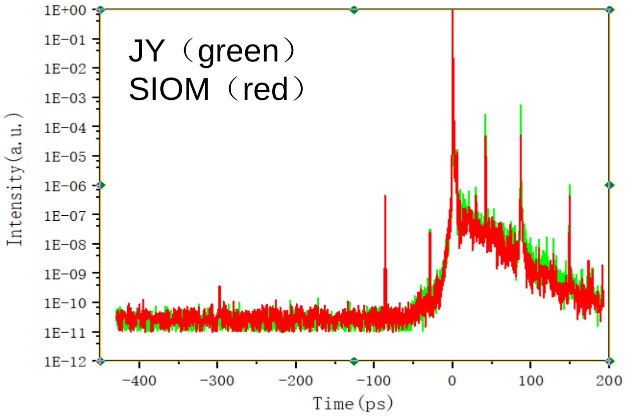

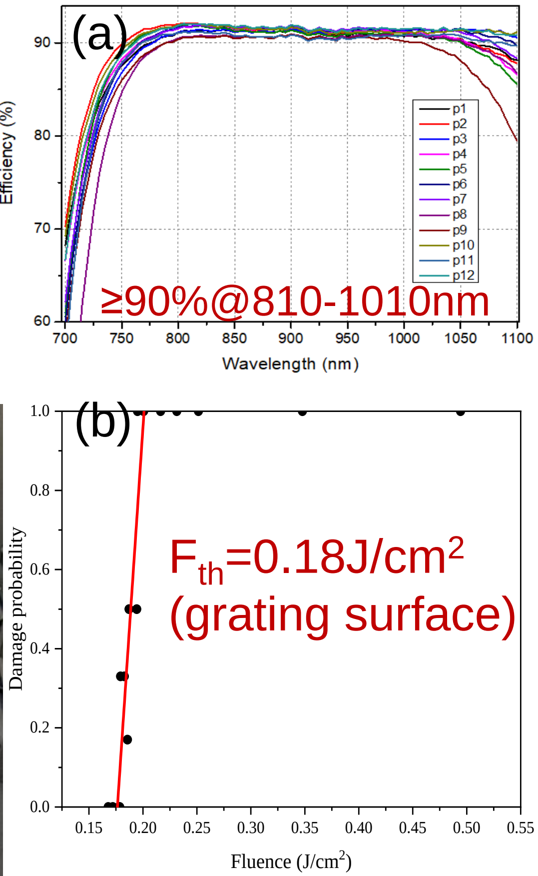

Fig. (a) Measured −1st-order diffraction efficiency; (b) LIDT.

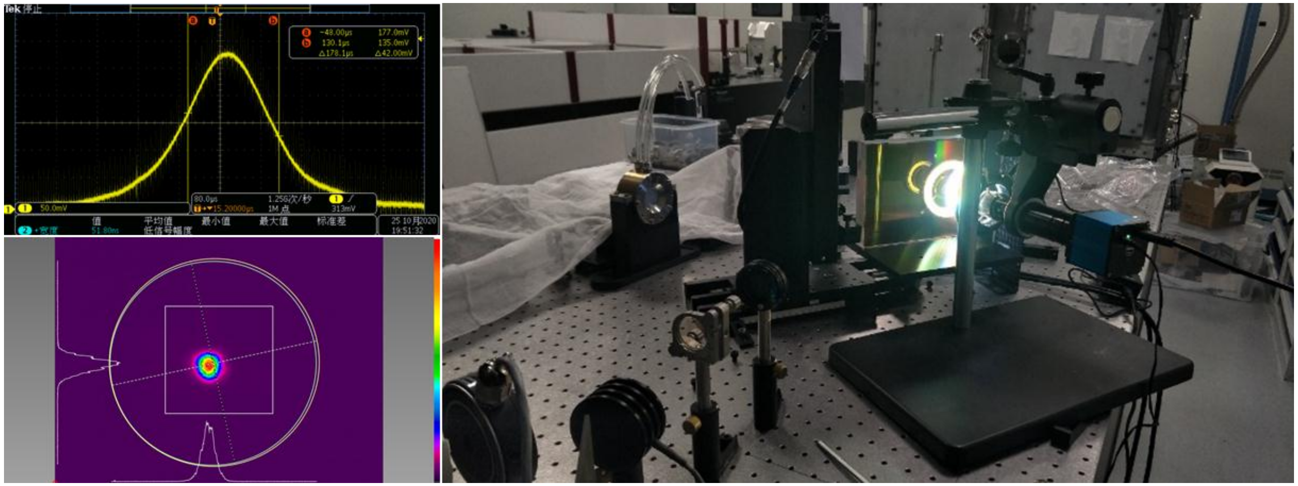

Fig. 200mm×150mm×25mm gold grating femtosecond pulse laser 1-on-1 test.

- September 20, 2020 @SIOM
- Excellent performances to address both engineering and scientific goals.

1400l/mm gold gratings

- 200mm×150mm

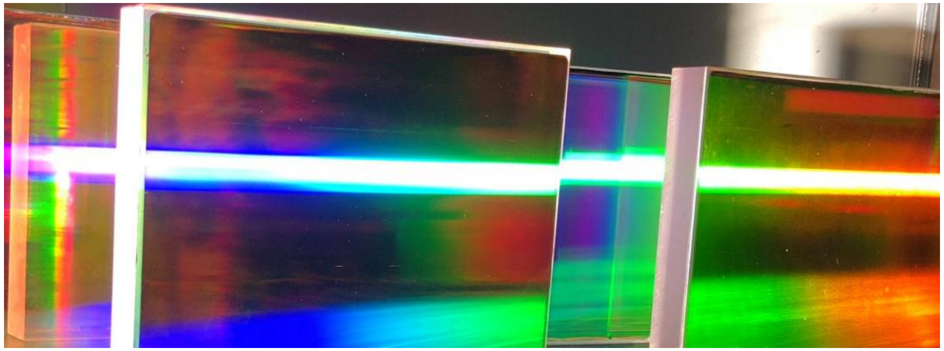

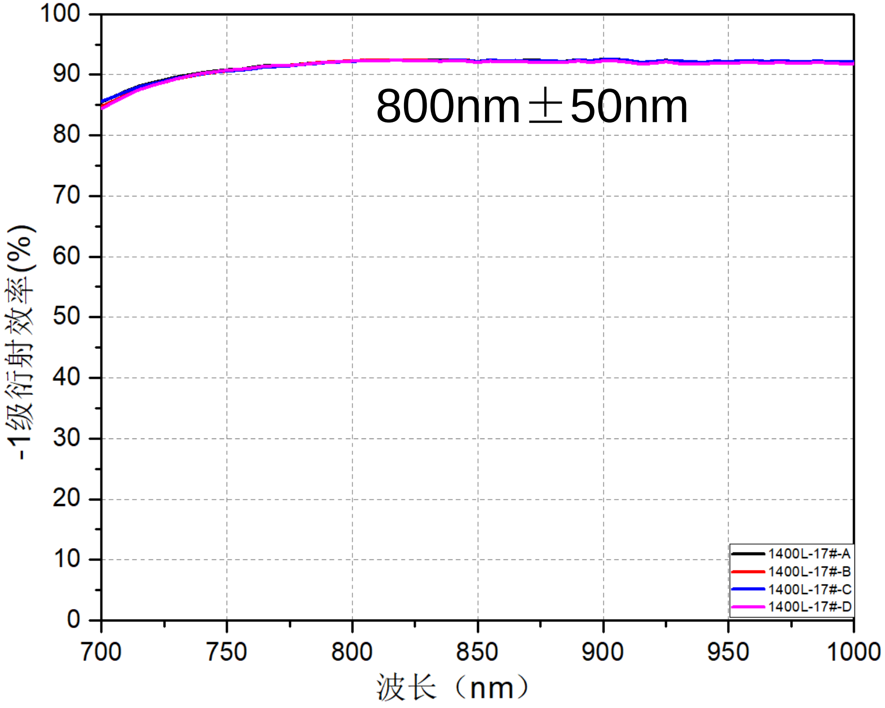

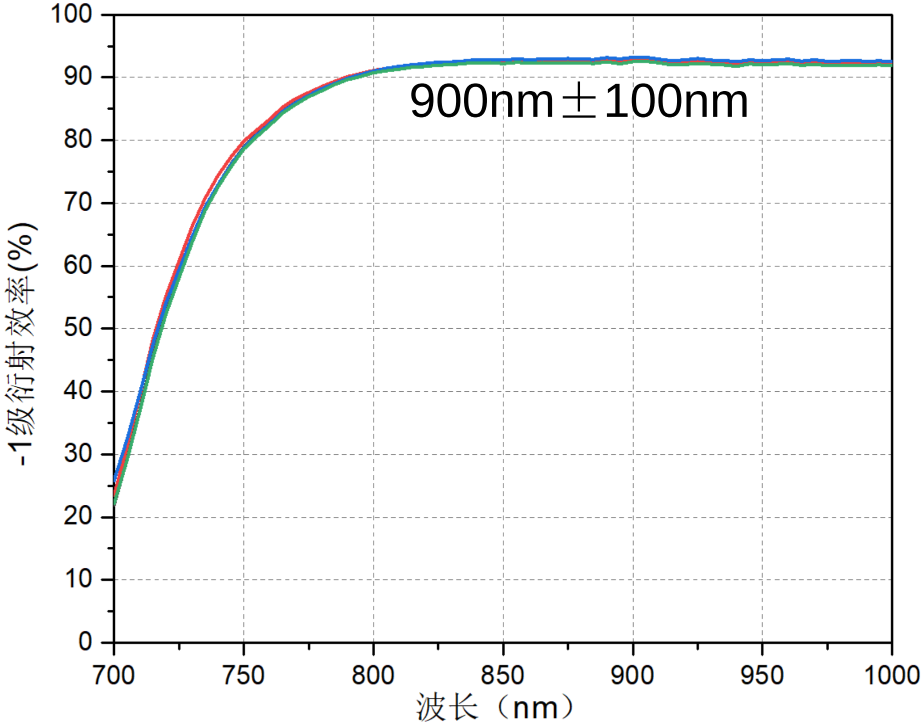

03

PART THREE

Gold-Dielectric Hybrid Gratings

Research progress

- @800nm and 1053nm

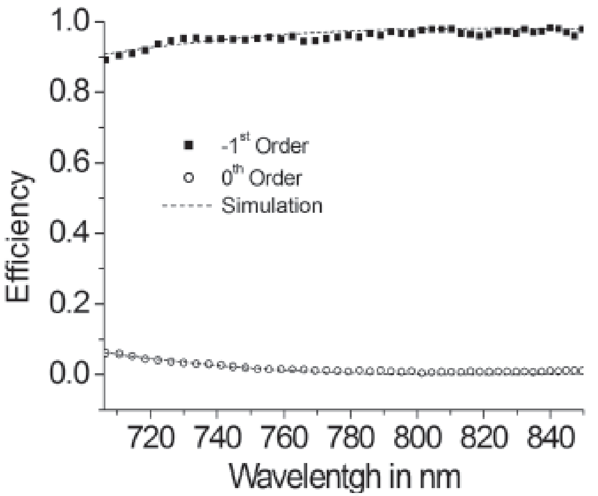

50fs	Damage Threshold (J.cm^{-2})	Diffraction angle (°)
Mixed Grating	1.1 ± 0.1	50
Dielectric Grating	1.1 ± 0.1	57
Dielectric multilayer	1.6 ± 0.2	57

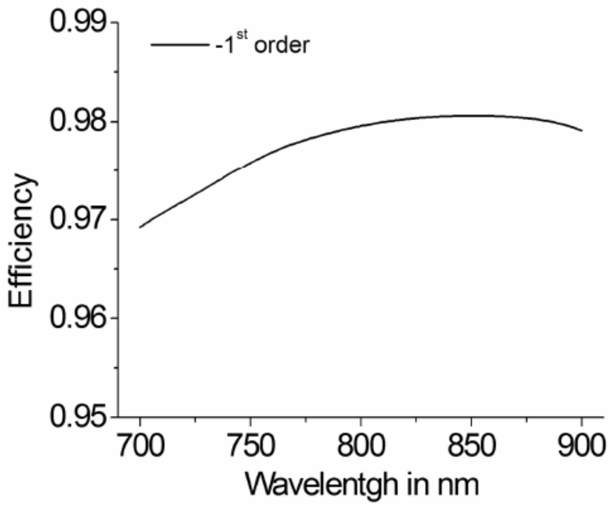

Damage threshold @1057nm, 500fs, 77.2°, beam normal (J/cm²)
2.79
2.27
3.24

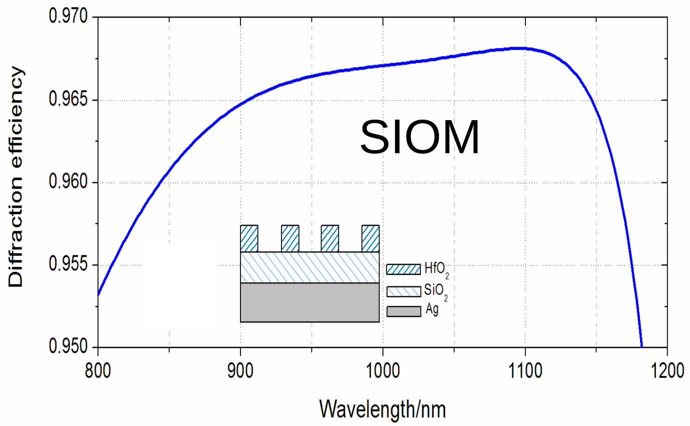

F. Canova, et.al, Opt. Express, 2007, 15: 15324-34, France;

D. H. Martz , et.al, Opt. Express, 2009, 17: 23809-23816,USA;

J.P.Wang,et.al, Opt. Lett.,2010,35:187-189, China

How to design the gratings

- Electromagnetics Module
- Optimization Module

Rigorous Coupled Wave Analysis (RCWA)

$$U^j(x,z)=\sum_m U_m^j \exp\{ik[\alpha_m x+\gamma(z-z_j)]\}$$

$$\{[\varepsilon]_{mn}-\alpha_{mn}^2\}[E_{ym}]=[\gamma_{mn}]^2[E_{ym}]$$

$$[H_{xm}]=[\gamma_{mn}][E_{ym}],[H_z]=\alpha_{mn}[E_{ym}]$$

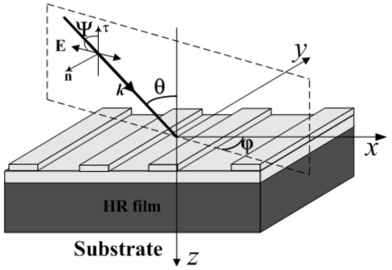

+

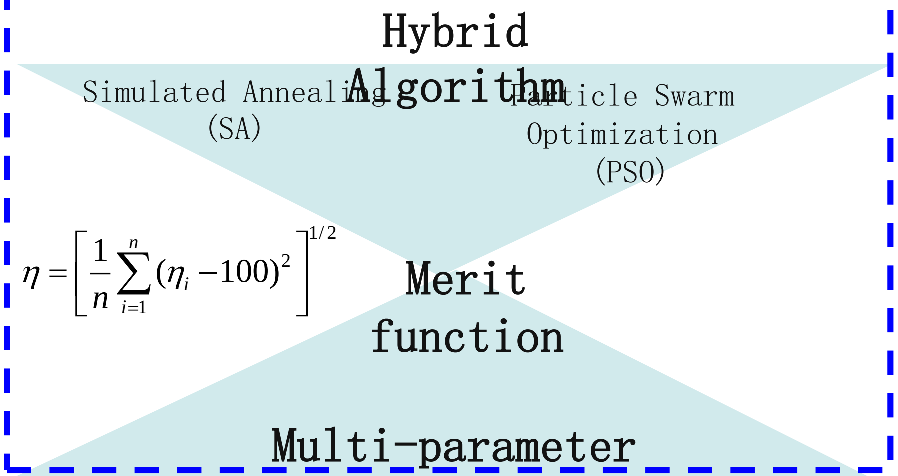

Hybrid Algorithm

Simulated Annealing (SA)

Particle Swarm Optimization (PSO)

$$\eta=\left[\frac{1}{n}\sum_{i=1}^{n}(\eta_i-100)^2\right]^{1/2}$$

Merit function

Multi-parameter optimization

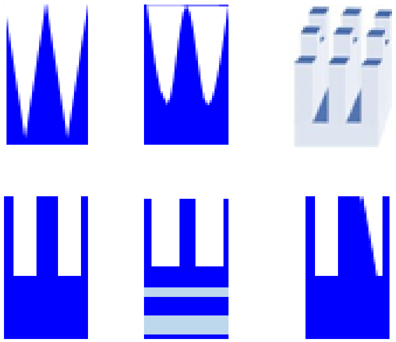

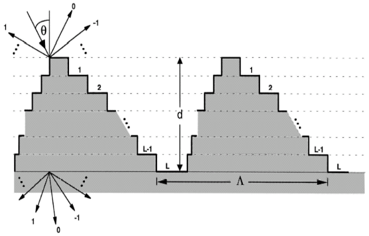

…

- ➢ Modulation shape (Depth/ Period/Duty cycle…)
- ➢ Application (Wavelength/ Angle/ Polarization…)
- ➢ Tolerance analysis

Opt Lett 35, 187-189 (2010)
Opt Lett 39, 170-173 (2014)
Opt Lett 42, 4016-4019 (2017)

- More accurate, more efficient, and more flexible methods.

Hybrid gratings type I

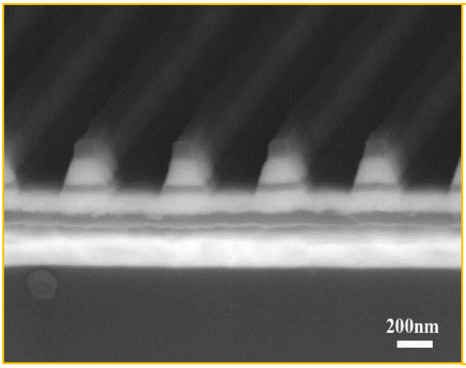

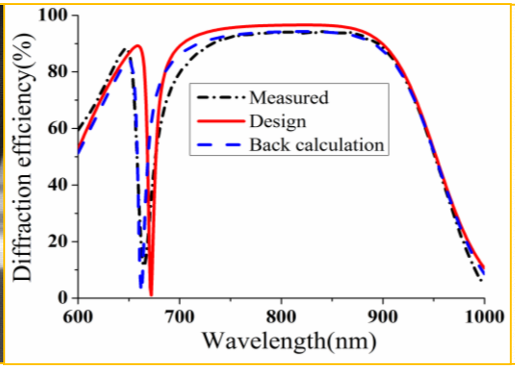

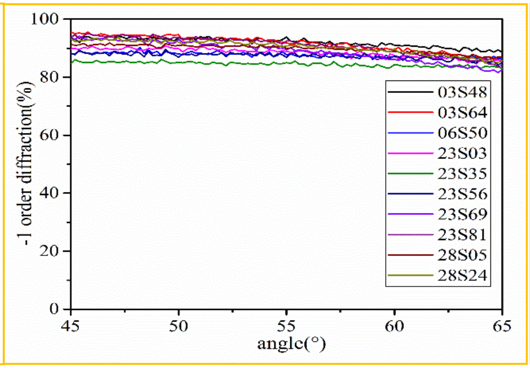

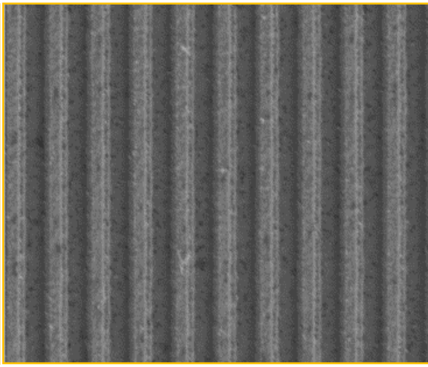

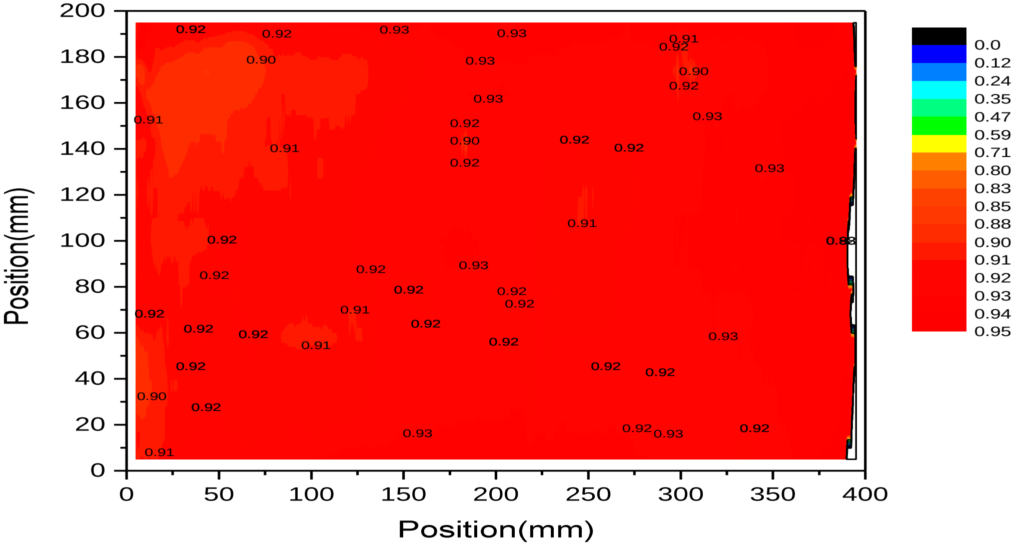

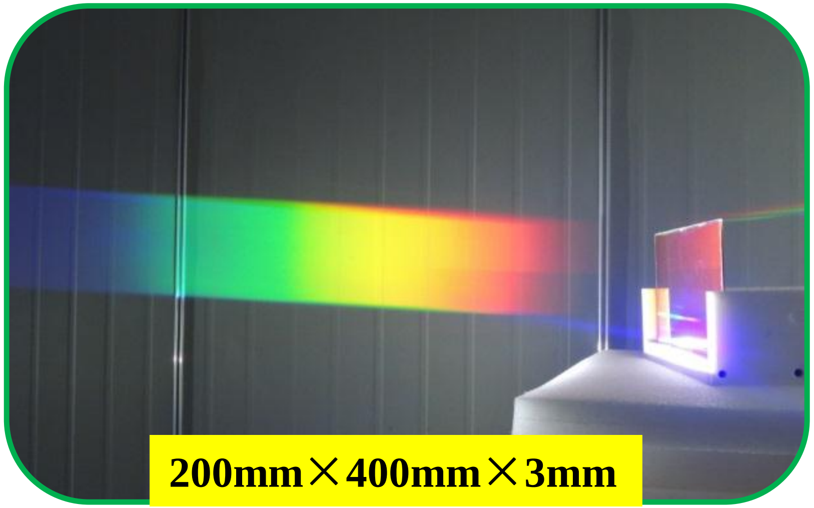

200mm×400mm×3mm

- Sandwich gratings structure@800nm±50nm,1740 line density

Laser induced damage morphology analysis

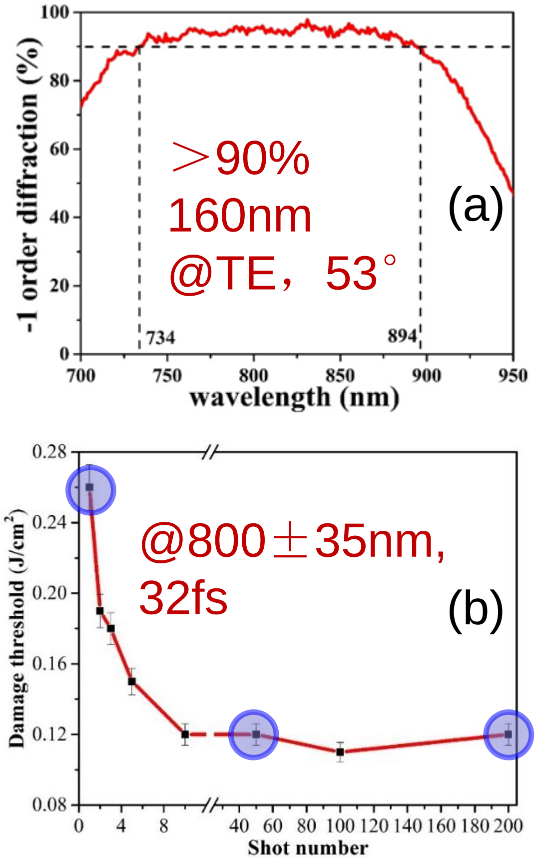

Fig. (a) Measured −1st-order diffraction efficiency;
(b) LIDT(on normal beam).

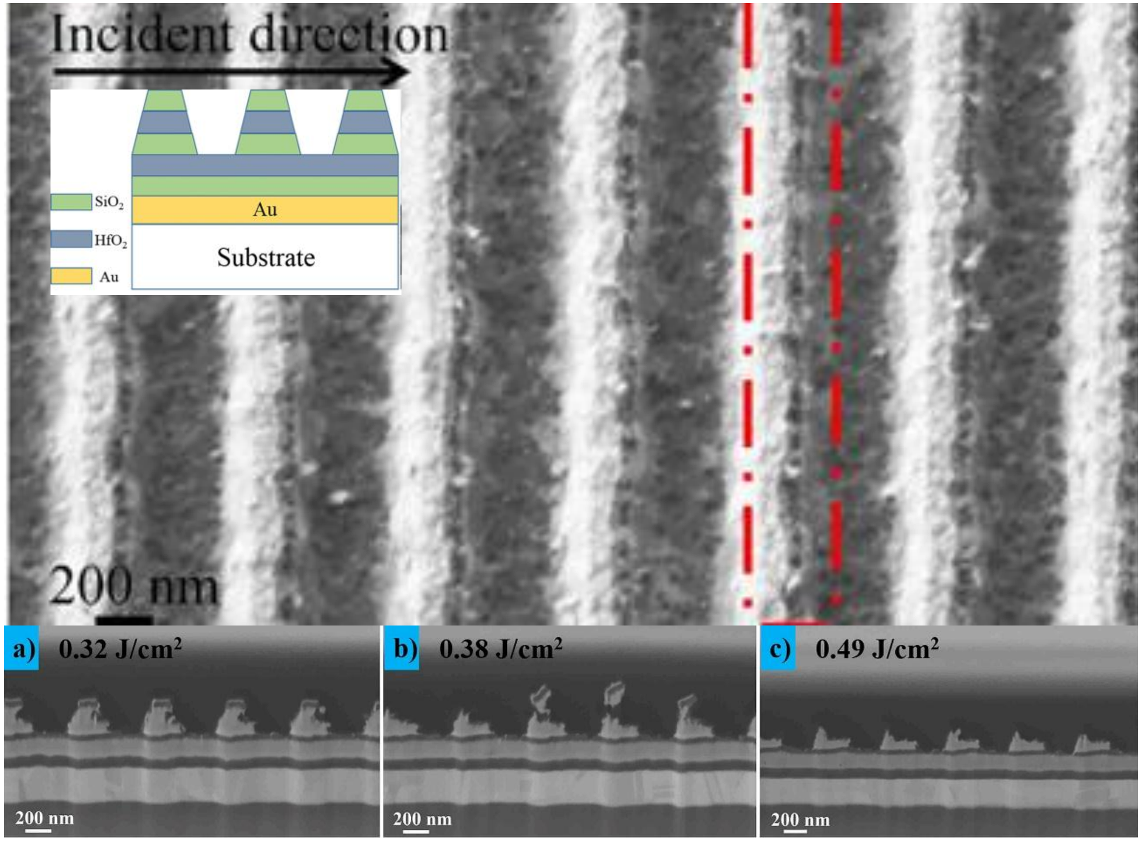

Fig. SEM images of typical damage morphologies near the damage threshold.
(a)(b)(c) Cross-sectional profiles of the damage spot at different laser fluences.

Optical Materials 75:727-732 (2018)

- Low LIDT (on grating surface @ 1-on-1) ~0.15J/cm^2;
- When S>10, LIDT (on grating surface @ S-on-1) ~0.12J/cm^2;
- The initial damage in HfO_2 layer of grating ridges opposite laser incidence direction.

Damage mechanism analysis

Optics & Laser Technology, 73:39-43(2015)

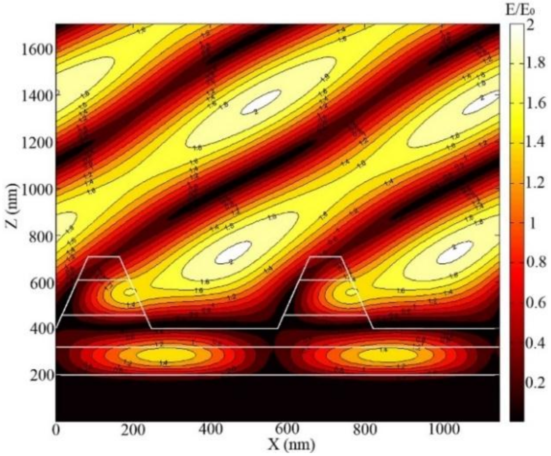

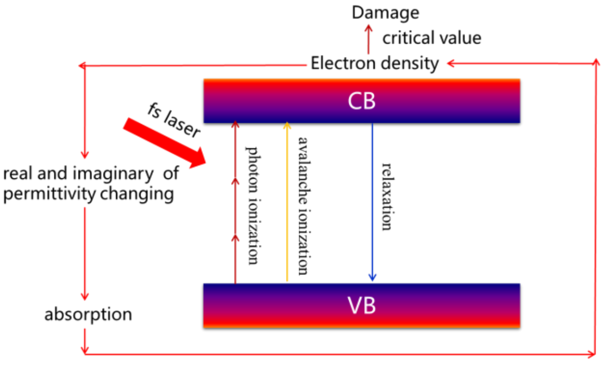

CB-Conduction Band; VB: Valence Band

Fig. Normalized electric field. The grating is illuminated from the left side at an angle of incidence of 53 in the TE polarization.

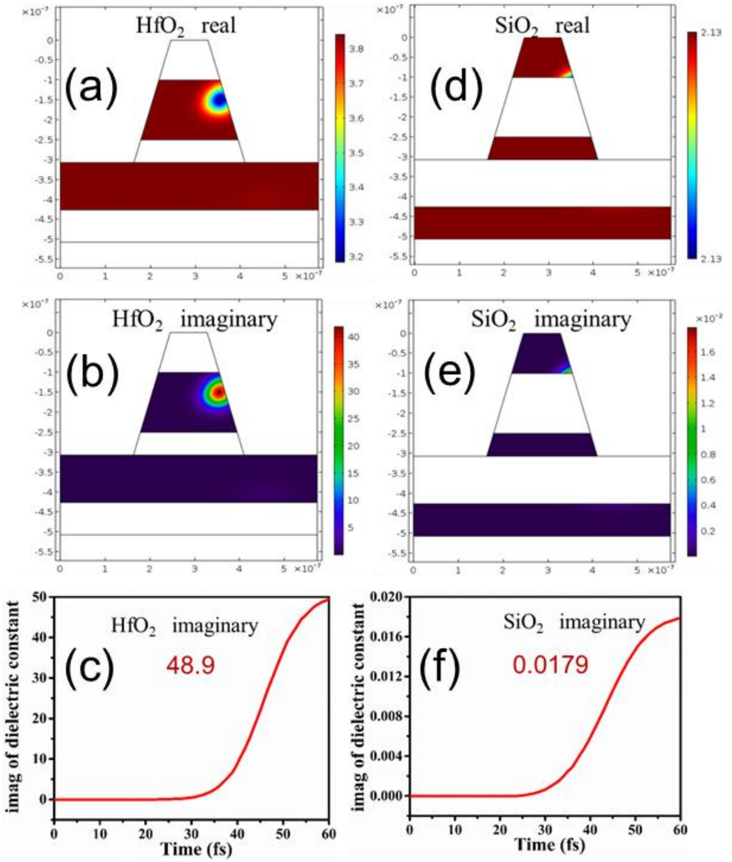

Fig. Dielectric constants of (a), (b) HfO2 and (d), (e) SiO2. Evolution of the imaginary parts of the dielectric constants of (c) HfO2 and (f) SiO2.

Opt. Mater. 75, 727-732 (2018)

- The reason of the low LIDT: the high NEFI and narrow bandgap of HfO_2.
- To design a new MMDG with SiO_2 grating lines.

Hybrid gratings type I I

Opt. Lett. 44, 2871-2874 (2019)

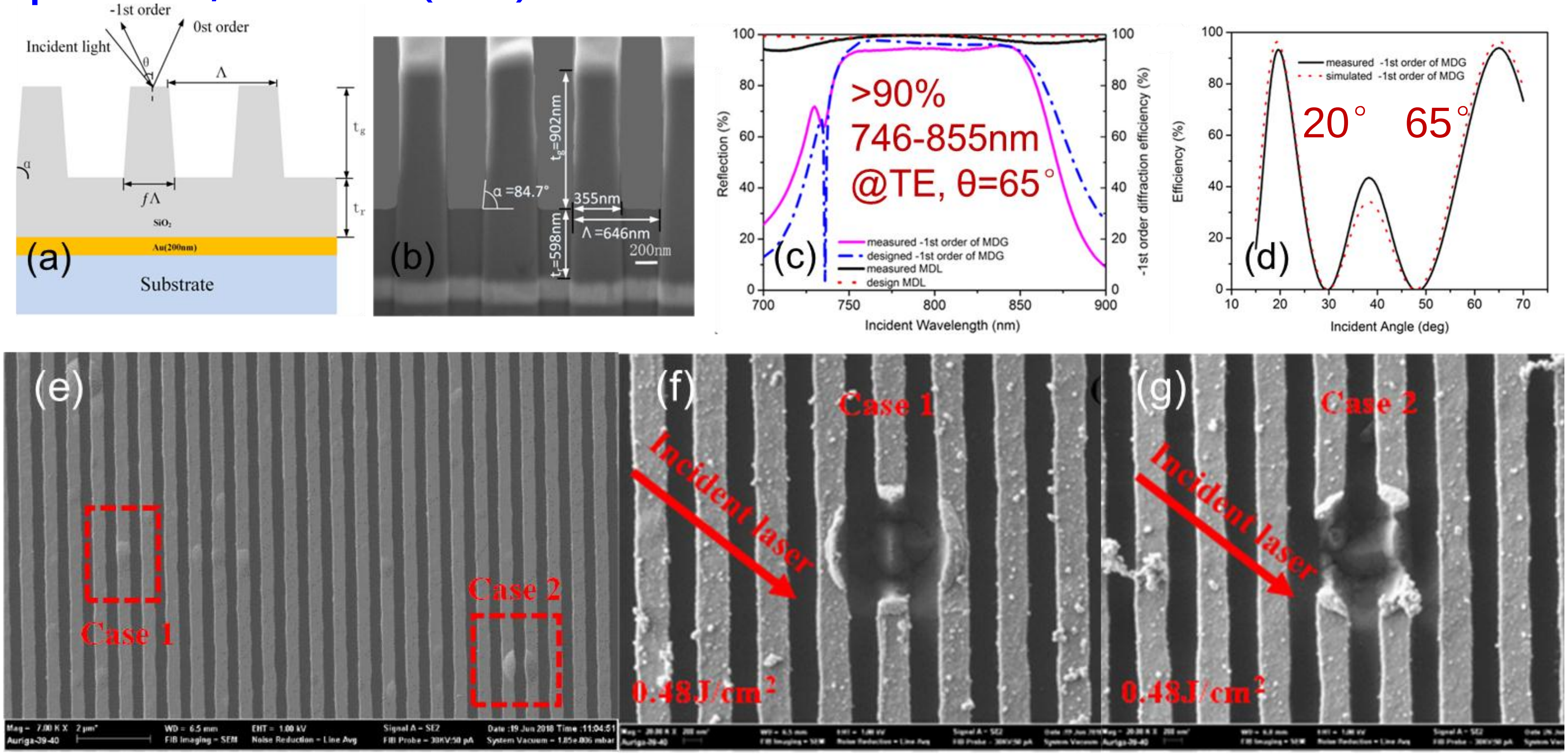

Fig. Gold-dielectric hybrid gratings type II. (a)Structure schematic; (b) cross-sectional image; (c) efficiency spectra; (d) angle spectra; (e) (f) (g) typical damage morphologies.

Opt. Mater. 91, 177-182 (2019)

- $\mathrm{LIDT}_{\mathrm{MMDG}}$(on grating surface @1-on-1)~0.4J/cm^2 ≈ 2×$\mathrm{LIDT}_{\mathrm{MG}}$(on grating surface @1-on-1);
- The initial damages: nodular defects.

Laser induced damage morphology analysis

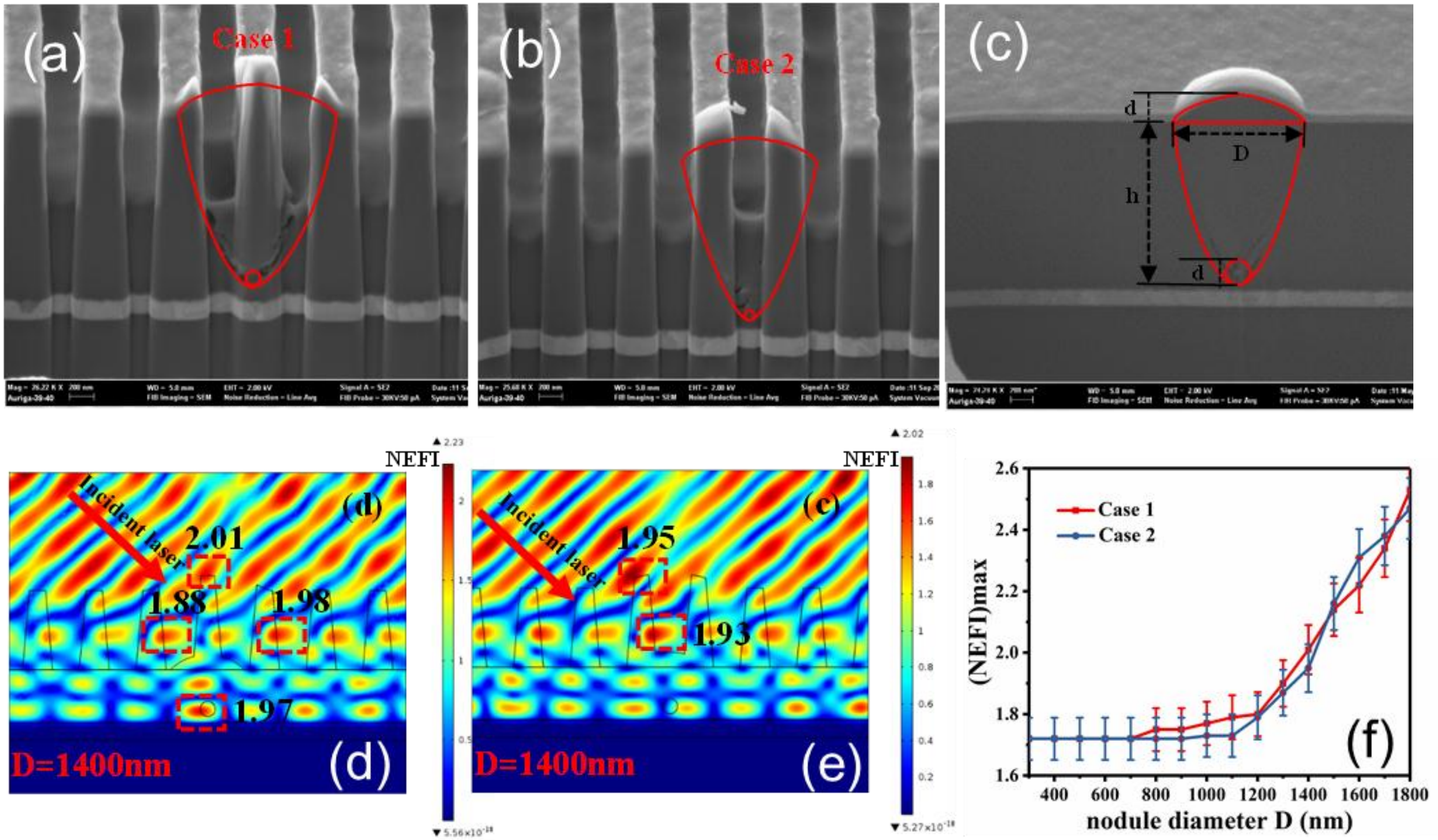

Fig. (a and b) The two cases of nodular defect; (C) the cross section of nodular defect in metal dielectric mixed film; (d) (e)NEFI distributions of case 1, case 2 when nodule diameter are 1400nm; (f) the evolution of maximum normalized electric field intensity (NEFI) with different nodule diameter in two cases.

Opt. Mater. 91, 177-182 (2019)

Opt. Lett. 44, 2871-2874 (2019)

- Significant NEFI enhancements in case 1 and case 2;
- The peak value of the NEFI increases rapidly once the size of diameter exceeds about 900nm.

Damage mechanism analysis

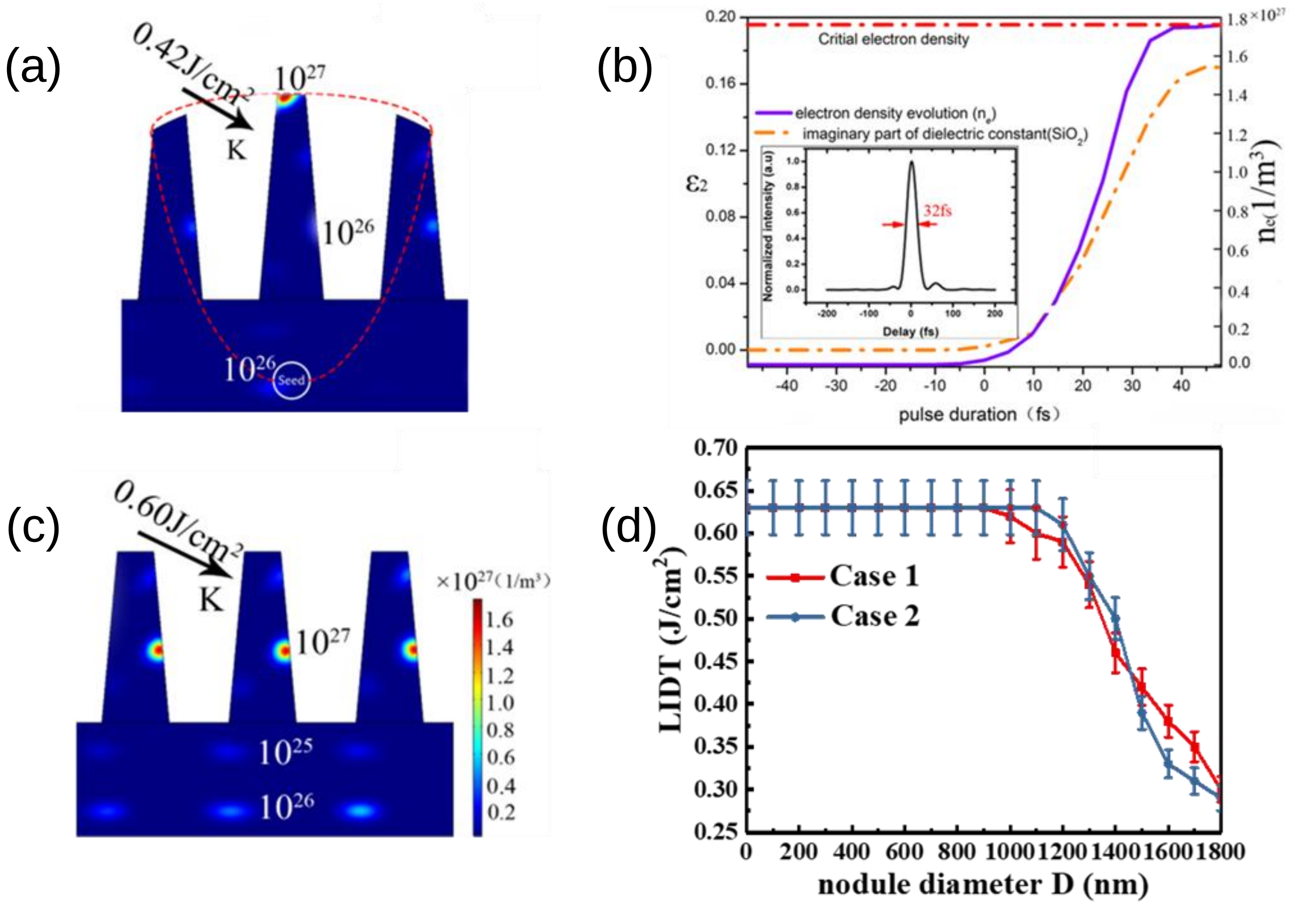

Fig. (a) n_e distribution in the SiO2 CB of the MDG with 1500nm nodule defect at the end of the pulse; (b) The evolution of electron density n_e in the CB and imaginary part of dielectric constant ε_2 of SiO2 in the MDG with a 1500nm nodule defect (0.42J/cm2, 32fs); (c) the electron density distribution in SiO2 CB of the perfect MDG (0.60J/cm2, 32fs); (d) the LIDTs of MDMG with different nodule diameters in two cases.

Opt. Lett. 44, 2871-2874 (2019)   Opt. Mater. 91, 177-182 (2019)

- By avoiding nodule defects or controlling the size of the nodulars in MMD deposition process.

LIDT of Hybrid Gratings and Gold Gratings group

Sample	Incident	Pol.	Normal(J/cm^2)	Grating(J/cm^2)
MMDL1#	65°	S	1.14	0.48
MMDL2#	65°	S	1.09	0.46
HG-1	65°	S	0.94	0.40
HG-2	65°	S	0.93	0.39
HG-3	65°	S	0.85	0.36
Sandwich	54°	S	0.28	0.17
MG-1	54°	P	0.32	0.19
MG-2	54°	P	0.35	0.21
MG-3	54°	P	0.39	0.23

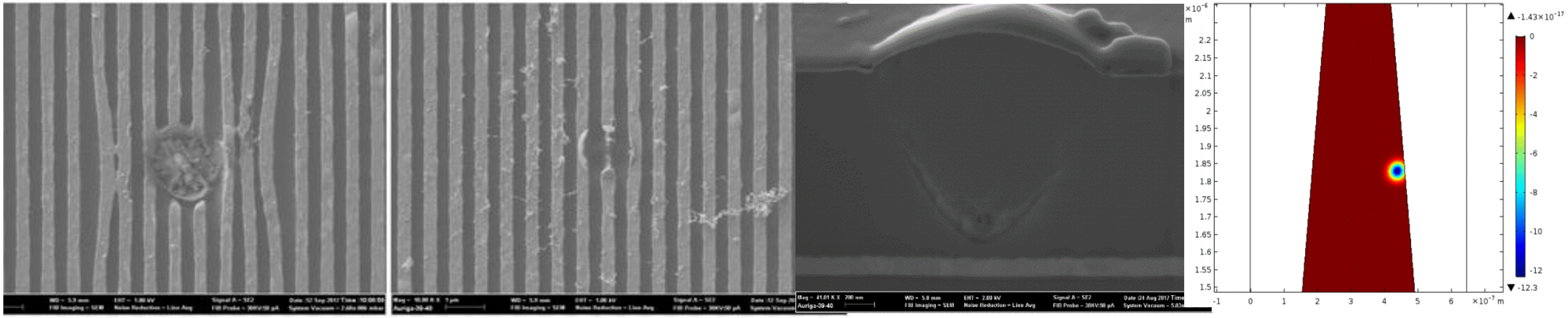

Enviroment for gratings fabrication

Clean room, ±0.08° C

Preparation for handle of large optics

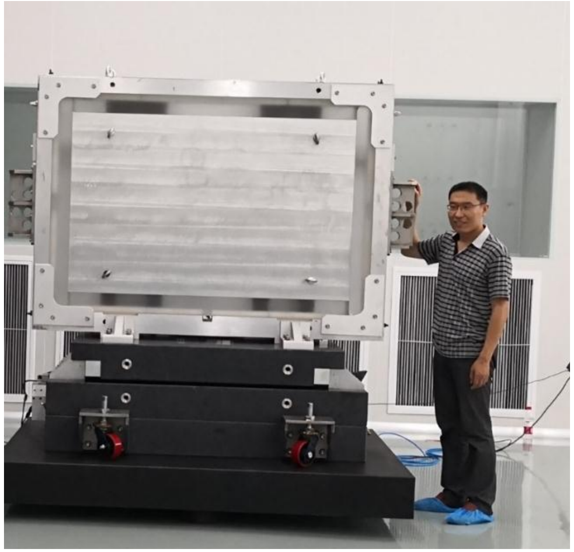

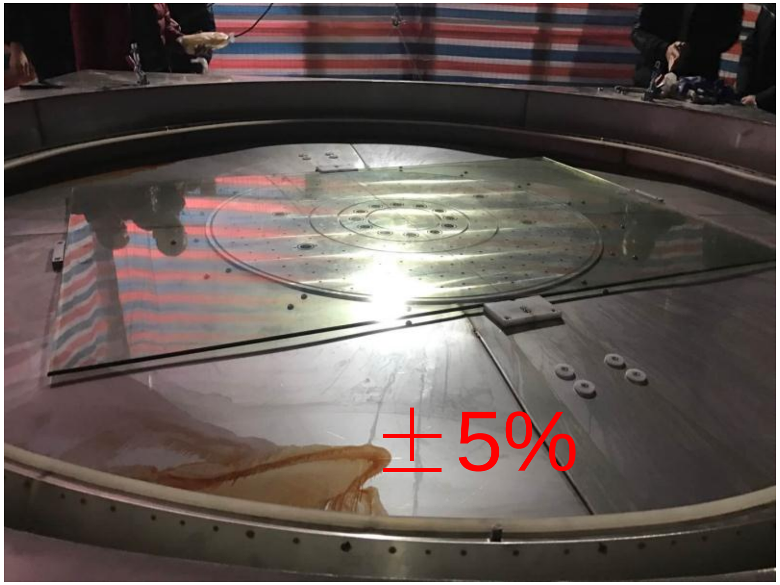

04

PART FOUR

Conclusion

HPG R&D system

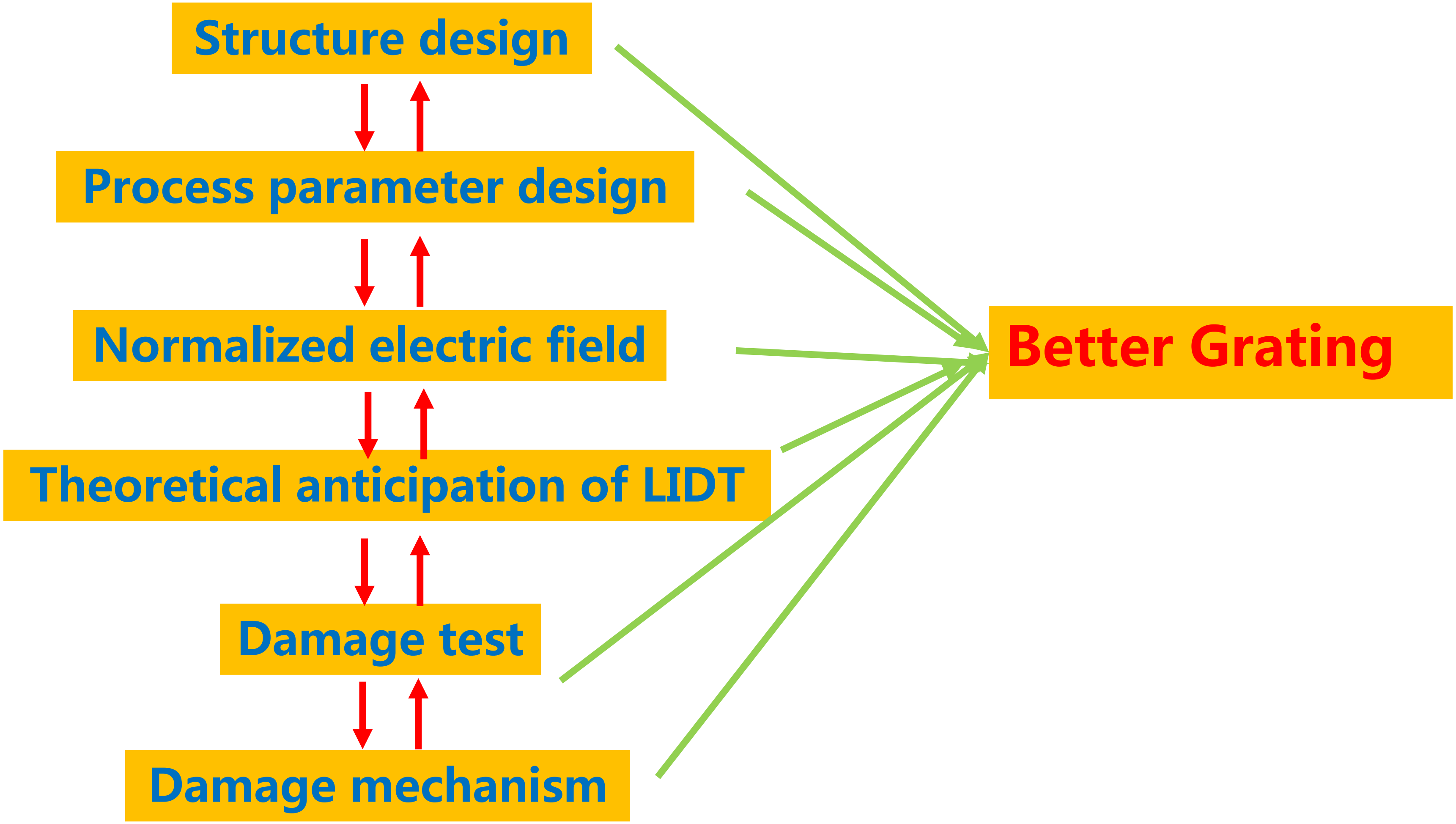

Structure design

Process parameter design

Normalized electric field

Theoretical anticipation of LIDT

Damage test

Damage mechanism

Better Grating

Future：higher power/high energy/shorter pulse

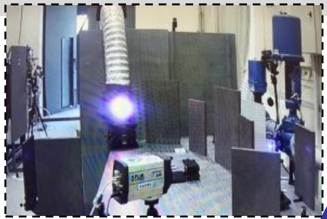

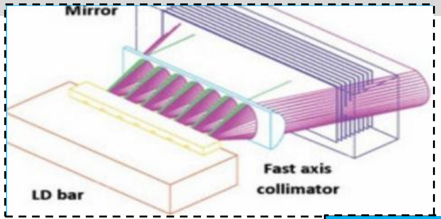

SAFETY

MEASUREMENT

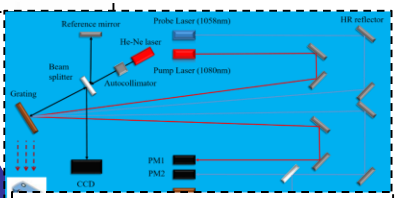

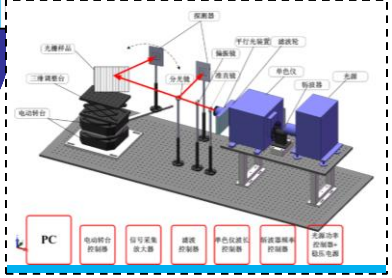

DESIGN

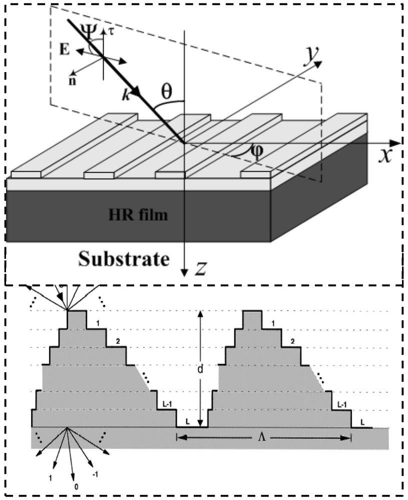

HPG

MATERIALS

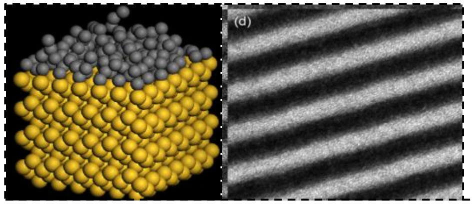

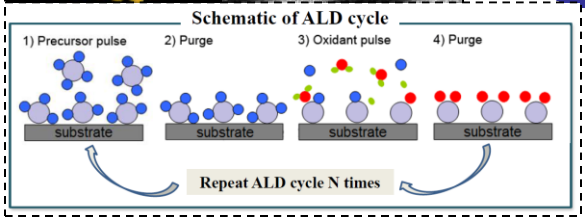

PROCESSING

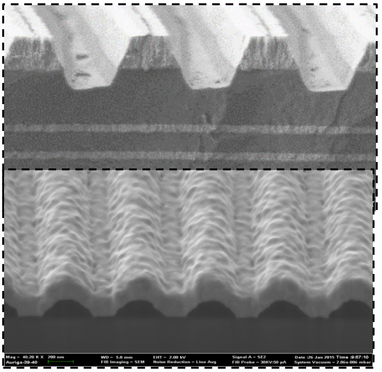

OPTICS

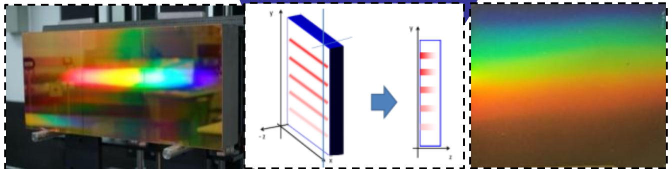

Thanks for your attention !